Cancer Stem Cell-Related Markers in Normal and Neoplastic Oral Mucosa

A study on human samples and experimental models

Tarig Al-Hadi Osman

Dissertation for the degree philosophiae doctor (PhD)

at the University of Bergen

2014

Dissertation date: June 4th, 2014

Scientific environment

1- The project had been carried out at Gade Laboratory for Pathology, Department of Clinical Medicine, Faculty of Medicine and Dentistry, University of Bergen.

2- The patient material was collected at Haukeland University Hospital, Bergen and University Hospital of North Norway (UNN), Tromsø, Norway.

3- Animal work was performed at the Laboratory Animal Facility, Faculty of Medicine and Dentistry, University of Bergen.

4- The project involved collaborators from University of Tromsø (Prof. Lars Uhlin-Hansen and Dr. Oddveig Rikardsen from Tumor Biology Research Group), Queen Mary University of London (Prof. Ian C Mackenzie and postdoc Adrian Biddle, Stem Cell Initiative Research Group and lecturer Muy-Teck Teh, Oral Biology Research Group).

Acknowledgements

First, Praise be to God, the Most Gracious, Most Merciful, who granted me with more blessings than I could ever count.

I would like to thank University of Bergen, The Quota program and the Norwegian Educational Loan Fund for the opportunity. My Sincere thanks to my supervisors: Prof. Daniela Elena Costea and Prof. Anne-Christine Johannessen, for the endless support and the guidance throughout the path, I was really privileged to work with you. My appreciation and gratitude to my colleagues at Section of Oral Pathology for their contribution to this project, as well as the nice times we had together; to the academic and the administrative staff at Gade Laboratory for Pathology, and Center for International Health for their help with many aspects of my study period; my collaborators, it was very nice and easy to work with you. And to Prof. Bjørn Mæhle, Prof. A\Raouf Eloteibi, Prof. Rune Nilsen, Prof. Kamal Elnour Mustafa, Prof. Kamal Abbass, Dr. A\Nasir Gafar and the late Dr. Nadia Ahmed Yahia (R.I.P) for all the discussion, advices and support.

Special thanks to everyone who has helped me during my field period in Sudan, although the project is not finished yet. The study participants, The Faculty of Dentistry- University of Khartoum; Institute of Endemic Diseases and Department of Biochemistry at Faculty of Medicine-University of Khartoum; Khartoum Teaching Dental Hospital (specially to Prof. Ahmed Suleiman and all members of his unit), Ribat National Hospital, the Army Hospital and University of Science and Technology- Omdurman. Many thanks to the ones who were helping just because of me; Maha , Shihab, Mohammed Hassan, Hind, Ahmed Amin, Gunn Moss, Abusibah, Mohammed Omer, Mazen, Hamada, Ghanim, Ammar, Alshafei, Migdad and Zak, without you guys it would have never been possible to achieve this.

It has been a long journey through many difficult times, and it would have not been possible to come through without the support of the family and friends. My deepest gratitude to my parents, my sisters and my brother, my late aunt Laila (may she rest in

peace), my dearest Omnia (my wife and my best friend), my children Ahmed and Rahma, for always believing in me, praying for me and standing by me. The Sudanese community in Bergen, thanks a lot for being around from the first day, it would have been very difficult without you. Thank you my whole family, colleagues and friends in Sudan and Norway for all the encouragement and love that you have given to me.

List of abbreviations

ALDH	aldehyde dehydrogenase family
ALDH1	class one aldehyde dehydrogenases
ALDH1A1	isoform A1 of class one aldehyde dehydrogenases
AML	acute myeloid leukemia
BMI1	the transcription factor polycomb complex protein BMI1
CSC	cancer stem cell, cancer stem-like cell, tumor initiating cell, tumorigenic cell
DAB	3,3`-diaminobenzidine tetrahydrochloride
DMEM	Dulbecco`s modified Eagle`s medium
EMT	epithelial to mesenchymal transition
ESA	epithelial specific antigen
FACS	fluorescence activated cell sorting
IHC	immunohistochemistry
Ki-67	mindbomb E3 ubiquitin protein ligase-1
NHOM	normal human oral mucosa
NOD/SCID	non-obese diabetic/severe combined immunodeficiency
NSG	NOD/SCID interleukin-2 receptor gamma chain null
NOK	normal oral keratinocyte
OD	oral dysplasia

OKSC	oral keratinocyte stem cell
OSCC	oral squamous cell carcinoma
p75NTR	the low affinity nerve growth factor
PcG	polycomb group proteins
qRT-PCR	quantitative reverse transcription polymerase chain reaction
SP	side population
TA	transit amplifying cells

Summary

The existence of cancer stem cells (CSCs) in solid cancers is still a controversial issue. Several markers were successfully used to enrich for cells with stem cell-like properties in oral squamous cell carcinoma (OSCC). Among these, ALDH1 was reported in both OSCC and several other human cancers. The aim of this study was to investigate the pattern of expression of several CSC-related markers including ALDH1 and the normal oral keratinocyte stem cell marker p75NTR relative to each other in patient samples and OSCC-derived cells, and the potential of p75NTR to identify and isolate CSCs in OSCC.

To simultaneously detect several CSC-related markers in patient samples, a multiple IHC protocol engaging three un-conjugated monoclonal primary antibodies from the same Ig subclass was first developed, based on previously reported protocols. Compared to other methods, stripping of the preceding reaction by microwave heating, combined with additional suppression of enzyme activity, has enabled specific detection of all three reactions by using the same detection system, with no detectable cross reactivity. Archival formalin-fixed paraffin embedded tissues from OSCC (n=177), oral dysplasia (OD, n=10), and normal human oral mucosa from healthy donors (NHOM, n=31) have been subjected to the developed multiple IHC protocol, while keratinocytes derived from OSCC, OD and NHOM were subjected to multiple fluorescent activated cell sorting (FACS). The findings of the two approaches showed a wider range of variability in the level of expression and localization of the CSC-related markers in OSCC and OD as compared to NHOM. In addition, the data also indicated a functional difference between different cellular phenotypes positive for either p75NTR or ALDH1A1. Firstly, higher proliferation (Ki67) was observed in p75NTR+ cells in comparison to ALDH1+ or p75NTR+ALDH1+ cells. Secondly, the frequency of p75NTR+ cells was higher in OSCCs of small size (T1 & T2) and OSCCs with poor to moderate differentiation grade, and correlated with poor survival of patients clinically deemed as of better prognosis. High frequency of ALDH1+ cells was found to be associated with lymph node metastasis. No statistically significant association was found between any of the clinical variables investigated and the

frequency of the co-localization of CSC-related markers. Thirdly, OSCC cells sorted for p75NTR and ALDH1 displayed different expression profile of several CSC-EMT related genes.

OSCC-derived cells sorted for p75NTR expression were compared for stem cell properties using both *in vivo* and *in vitro* assays. Statistically significant higher stem cell properties were found for the $p75NTR^{High}$ cells than for the $p75NTR^{Low}$cells in all assays performed. This suggested that p75NTR can be used for isolating a subpopulation enriched for cells with stem cell–like properties in OSCC. Nevertheless, the $p75NTR^{Low}$ subpopulation did also exhibit some stem cell features, but to a lesser extent. Propagation of $p75NTR^{Low}$ cells for several passages in culture showed that the expression of p75NTR could rise spontaneously. This finding was also supported by the similar expression of p75NTR by the xenografts generated by both subpopulations in NOD\SCID IL2Rɤnull mice. Similar spontaneous generation of $ALDH1^{High}$ cells by propagation of $ALDH1^{Low}$ cells was observed, although with a different kinetic.

Taken together, the data from this study showed high inter-patient variability in the expression of the CSC markers investigated, and high intra-tumor heterogeneity of the CSC subpopulation. The results presented here suggest also that some OSCC might have several distinct CSC phenotypes, each with impact on different clinical aspects, while other OSCC might completely lack a hierarchical organization. *De novo* generation of $p75NTR^{High}$ or $ALDH1^{High}$ cells from their negative counterparts might indicate the existence of a dynamic equilibrium between cancer cells with different degrees of differentiation.

List of publications

I. Successful triple immunoenzymatic method employing primary antibodies from same species and same immunoglobulin subclass.

T.A. Osman, G. Øijordbakken, D.E. Costea, A.C. Johannessen, European journal of histochemistry : EJH 2013; 57: e22.

II. Multiple Immunostaining Identifies Separate Cancer Stem Cell Subpopulations in Oral Squamous Cell Carcinoma

Tarig A. Osman, Oddveig Rikardsen, Muy-Teck Teh, Dipak Sapkota, Xiao Liang, Evelyn Neppelberg, Adrian Biddle, Ian Mackenzie, Lars Uhlin-Hansen, Anne Ch. Johannessen, Daniela E. Costea, (Manuscript)

III. p75NTR, a marker of normal oral keratinocyte stem cells, identifies a transient stem cell state of oral squamous cell carcinoma cells.

Tarig A. Osman, Himalaya Parajuli, Dipak Sapkota, Anne Ch. Johannessen, Daniela E. Costea, (Submitted Manuscript)

Contents

1. Background

1.1 Oral epithelium: from normal homeostasis to carcinoma

1.1.1 Histology and tissue architecture of normal human oral mucosa

Oral mucosa is the moist lining of the oral cavity that is continuous with the skin at the lips, and the gut lining at the larynx. Like the other mucous membranes in the human body, the oral mucosa is composed of stratified squamous epithelium, and underlying connective tissue. The epithelial component is composed of different layers (strata) of keratinocytes: basal cell layer/ stratum basale, prickle cell layer/startum spinosum, granular cell layer/stratum granulosum (present only in the hard palate) and superficial cell layer/stratum superficiale (Figure 1). The connective tissue component is composed of lamina propria and submucosa. The lamina propria indents the epithelium in a form of projections, known as connective tissue papilla, to provide blood and nerve supply to the adjacent avascular structure (1).

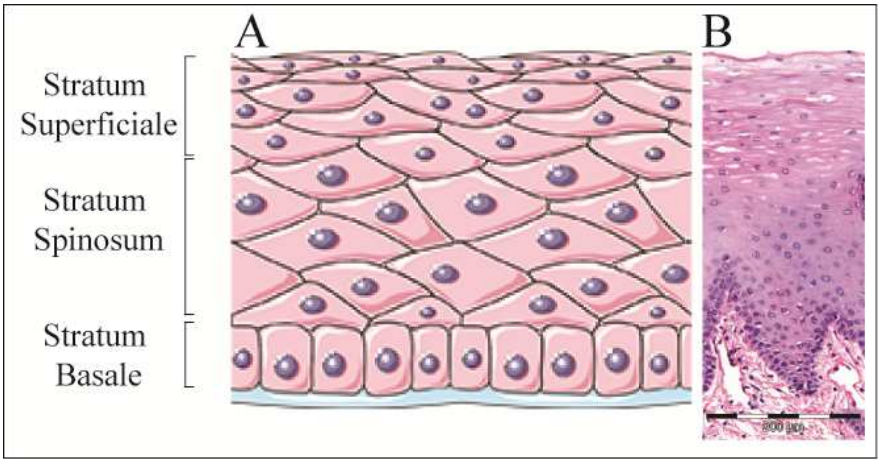

Figure 1: Schematic drawing illustrating different layers of the oral epithelium (A). Source: Servier Medical Art, http://www.servier.com/Powerpoint-image-bank.
Section from normal human buccal mucosa stained with H&E; own photo (B).

Oral mucosa is classified into three main categories: lining mucosa which is found around mobile structures, and has connective tissue rich in elastin; masticatory mucosa which covers the attached gingiva and hard palate, it is a rigid structure that is bound to the underlying bone by a dense connective tissue; and specialized mucosa that contains specialized mucosal structures like the taste buds present in the dorsum of the tongue (1).

1.1.2 Homeostasis of the normal human oral epithelium

In all multicellular organisms, the number of cells is maintained through the finely regulated balance between cell division, differentiation and programmed cell death (apoptosis) known as homeostasis (1, 2). Keratinocytes of the oral mucosa (NOKs) follow a distinct program in which they stop dividing, terminally differentiate, and shed off at the surface. The process involves acquiring characteristics necessary to the desired function, and partial activation of the apoptotic machinery, through sequential expression of different genes (3, 4). Keratinocytes are produced in the basal and parabasal cell layers by division of the stem cells and their direct progeny, the transit amplifying cells (TAs) (1). Stem cells of the oral mucosa reside within the basal layer in clusters that are located at the tips of the connective tissue papilla and the deep rete ridges, and have a slow cycling rate (5), while their actively cycling progeny (TA) migrates laterally and upwards, forming a clone-like pattern, and are cycling more rapidly (6). Differentiation process of the keratinocytes starts by breaking the attachment to the basal lamina (basement membrane), an important trigger of the maturation process. Keratinocytes are pushed up by the pressure generated by proliferation of the cells in the layers underneath (Figure 2), leading to the stratification of the tissue (1).

During their migration to the surface, oral keratinocytes follow one of two major scenarios. First scenario occurs at the surface of masticatory mucosae, where keratinocytes lose their nuclei and cytoplasmic organelles, and become filled with keratin forming a cornified layer (3), that is suitable for its desired function as a resilient barrier and a frictional withstander. In the second scenario terminal

differentiation does not include a cornification process; instead, it results in the more elastic barrier of the lining mucosae. Moreover, special forms of terminal differentiation are site specific, and result in the formation of epithelial appendages like the filiform papillae at the dorsum of the tongue. In all types of mucosa, the surface layer is regularly shed, and replaced by successors from the underlying layers (1).

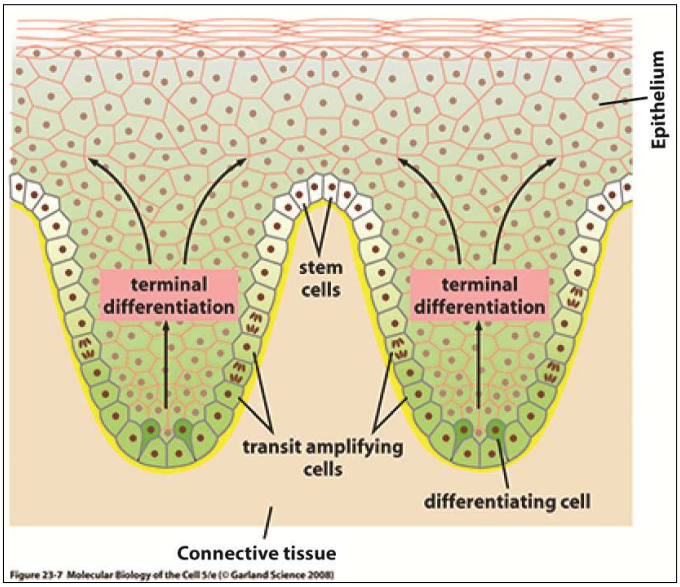

Figure 2: Schematic drawing illustrating upwards migration of differentiating keratinocytes, the localization of stem cells and transit amplifying cells; Source: Modified from: ALBERTS B, JOHNSON A, LEWIS J et al. Molecular Biology of The Cell. Garland Science: New York, 2008; 1600.

1.1.3 Stem cells

Stem cells are important players in tissue homeostasis, and are very unique in their ability of self-renewal and differentiation to various tissue specific lineages (4). The microenvironment of stem cells controls the balance between their self-renewal and differentiation capacities, and subsequently homeostasis of the organ is achieved. They are slow cyclers that normally remain dormant until they receive a stimulating signal

when their activity is needed, as during wound healing (4). When activated, stem cells have unlimited replicative potential and may divide asymmetrically to give rise to one stem cell that remains quiescent in the stem cell niche until another stimulating signal is received, and thus the self-renewal, while the other offspring being committed to differentiation (Figure 3). Stem cells may also divide in a symmetrical pattern either to reproduce two daughter cells both of which enter differentiation pathways, or two daughter stem cells, so as to maintain the stem cell pool like in situations of tissue loss by wounding. In comparison, transient amplifying cells are actively proliferative, but are destined for differentiation later during their life time (4). This hierarchical organization was shown in normal human oral mucosa, and has drawn attention as a possible cell source for tissue engineering and reconstructions (5).

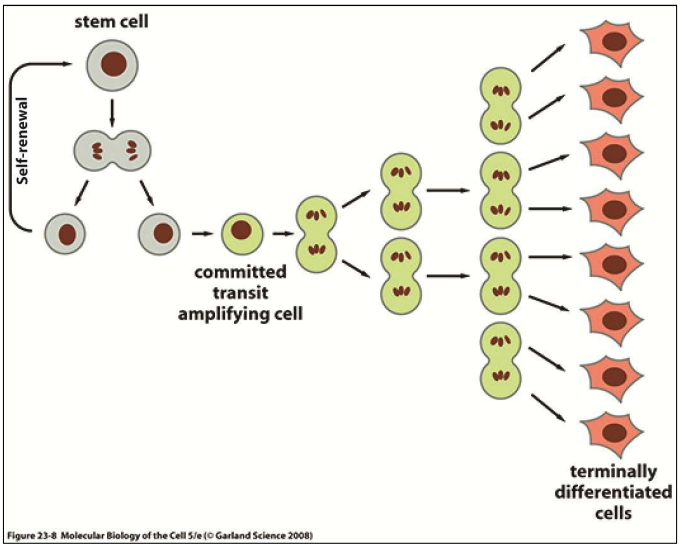

Figure 3: Asymmetrical division of stem cells resulting in one daughter stem cell and a committed transit amplifying cell. Source: ALBERTS B, JOHNSON A, LEWIS J et al. Molecular Biology of The Cell. Garland Science: New York, 2008; 1600.

1.1.4 The role of the microenvironment

As surface barrier, the epithelium has to adapt to tough circumstances, like wounding or continuous friction, and keep the surface properly covered while homeostasis is still maintained. This is achieved by modulating the proliferation rate of both TAs and stem cells, the fate of the stem cell progeny and the time for TAs to enter and complete the differentiation program. These processes are modulated, according to the needs, by a multitude of signalling molecules mediating the interaction of keratinocytes with each other, with other types of cells in their surroundings and with extracellular matrix components. For example, contact with the basal lamina was found to keep keratinocytes at the basal layer undifferentiated via integrins signalling, and basal keratinocytes grown in suspension stop dividing and start to differentiate (4). Both the stem cells and TAs respond to stimuli in their microenviroment to meet the tissue needs. As already mentioned, TAs start their differentiation program by getting unleashed from the basal lamina, and migrate up to the parabasal compartment. On the other hand, the microenvironment of the stem cells, often called the stem cell niche, is apparently essential for them to remain in an undifferentiated state (4).

1.1.5 Molecular control of stemness and differentiation

During differentiation, progenitor cells become committed to a specific lineage, and expression of genes required for differentiation into other lineages become restricted. These restrictions become inheritable through epigenetic modifications to the DNA that serve as cellular memory of lineage commitment (7). On the other hand, stem cells have gene expression potential that enables them to differentiate into various tissue lineages (7), an ability referred to as cell potency. The self-renewal capacity of stem cells renders them permanent residents of the tissue, by maintaining at least a daughter cell in an undifferentiated state. Substantial knowledge of the regulatory circuit is so far lacking, but several transcription factors, including Oct4A, SOX2, c-myc and Klf4 and NANOG, have been found to promote both self-renewal and pluripotency in embryonic stem cells (8, 9). In addition, other molecular mechanisms have been described to be involved in maintain the hierarchy of the tissue.

Polycomb group proteins (PcG)

Members of this group repress the expression of some genes by exerting epigenetic modifications in the targeted genes, which have to be reversed upon differentiation (2, 7). They have been named “the guardians of stemness” because many of their targeted genes were found to promote differentiation (2). However, human DNA mapping revealed that some of the targeted genes carry both repressive and activating PcG mark, comprising a bivalent domain (7). Accordingly, binding to the bivalent domain comprises a cell fate decision, and PcG contributes to stem cell pluripotency by postponing lineage commitment (7). In addition, the PcG members BMI1 was found to be essential in self-renewal of mammary and hematopoietic stem cells (10, 11). BMI1 also functions as a transcriptional repressor of two tumor suppressor genes, P16ink4a and P14Arf. The first is a cyclin-dependent kinase inhibitor while the later promotes apoptosis and cell cycle arrest (4, 12).

Wingless (Wnt) signalling Pathway

Tcf/LEF family of transcription factors regulates, among others, several genes involved in the cell cycle control (e.g: c-myc, cyclin D and adhesion molecules from the EPH family). B-catenin, an important component of the adherence junction, is made available and accumulates in the nucleus when Wnt pathway is activated (13). B-catenin serves as co-activator of Tcf/LEF family of transcription factors. A degradation complex composed of proteins, and located in the cytoplasm, can molecularly flag B-catenin for degradation by the proteasome (Figure 4A). This degradation complex includes axin, APC, GSK3B and CKI. Wnt signaling pathway disrupts the degradation complex mentioned above by recruiting the axin by one of the pathway mediators (phosphorylated LRP, Figure 4B). Research have shown that Wnt pathway is required for self-renewal of neural (14, 15), intestinal and haematopoetic (16) stem cells.

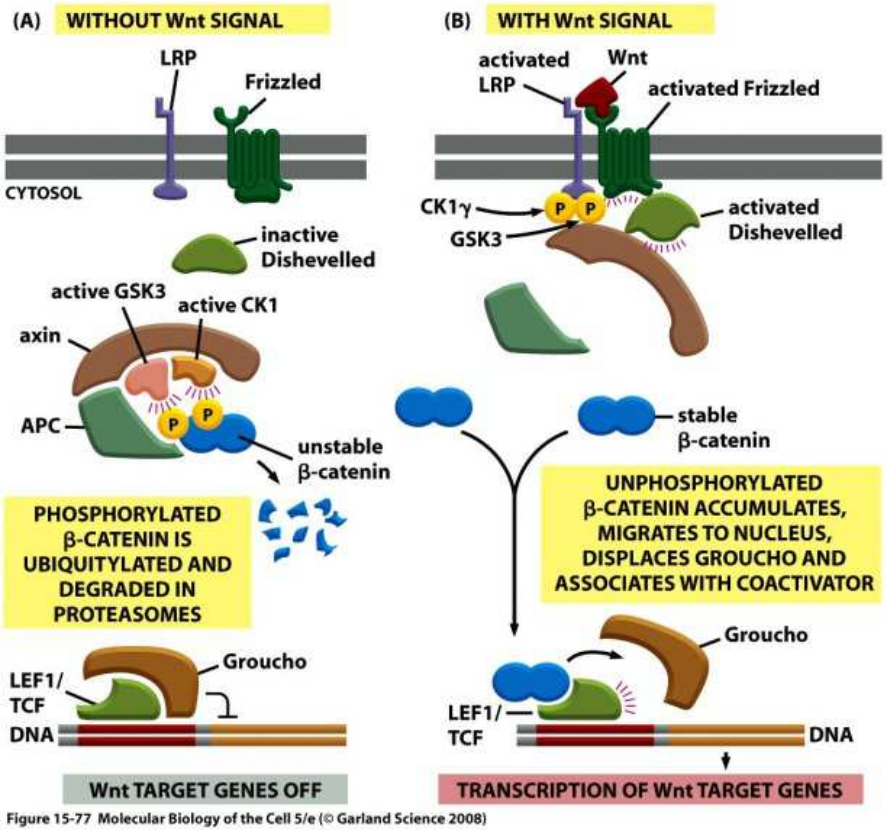

Figure 4: Wnt signaling pathway. Recruitment of β-catenin by the cytoplasmic degradation complex (A), β-catenin made available by disruption of the degradation complex (B). Source: ALBERTS B, JOHNSON A, LEWIS J et al. Molecular Biology of The Cell. Garland Science: New York, 2008; 1600.

Hedgehog pathway (Hh)

Hedgehog pathway is another pathway that seems to be involved in self-renewal (2, 10). The signal transduction is mediated by two transmembrane molecules, Patched and Smoothened. In the absence of the Hh ligands (Figure 5A), patch inhibits Smoothened and suppresses the pathway. The signal is transduced upon relieve of this inhibition by binding of patched to the ligand (Figure 5B). Although the rest of the signaling cascade has not been fully elucidated, it involves the release of the zinc finger transcription factor Gli from a protein complex to facilitate its translocation to

the nucleus (2, 10). The isoform Gli2 was found to promote self-renewal of mammary progenitor cells by modulating the expression of BMI-1 (10).

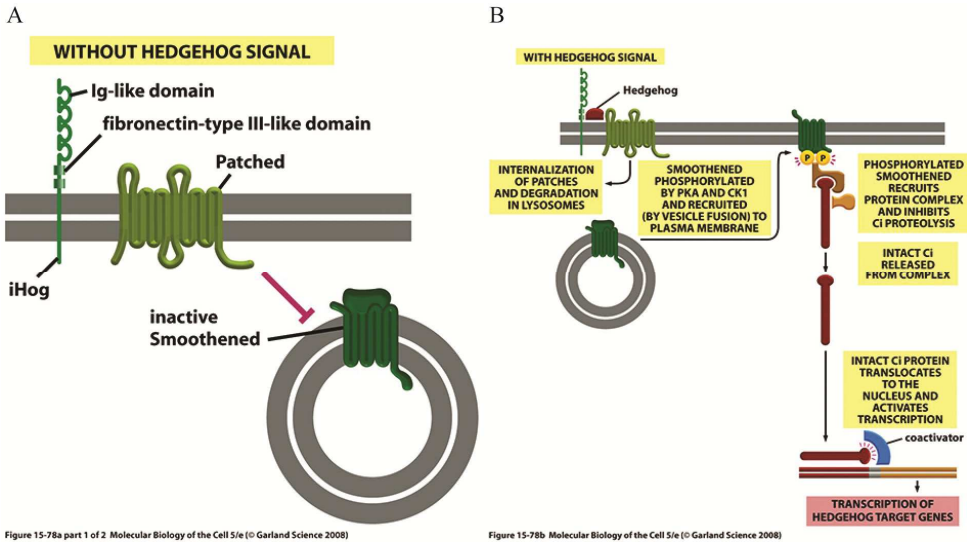

Figure 5: Inhibition of Smoothened by Patched in the absence of Hodgehog signal (A), Phosphorylation of Smoothend and internalization of Patches and activation of the pathway upon ligand binding. Source: ALBERTS B, JOHNSON A, LEWIS J et al. Molecular Biology of The Cell. Garland Science: New York, 2008; 1600.

Notch pathway

Notch pathway plays an essential role in cell fate decision in nearly all developing tissues (4, 17), and was found involved in both stem cell fate and maintenance in embryonic (18) and adult (19, 20) stem cells. The pathway is triggered by binding of any of the Delta-Serrate-LAG2 (DSL) ligands from one cell, to the transmembrane receptor notch in a neighboring one. This binding results in cleavage of notch cytoplasmic tail, and subsequent translocation to the nucleus (Figure 6). The cleaved cytoplasmic tail participates in core transcriptional complexes, and thus aids in transcription of targeted genes (4, 17). The genes regulated by notch signaling were found to promote variable cellular processes during development, depending on the tissue and biological circumstances (4, 17). The pathway plays a role in limiting the

number of stem cells, by inducing neighbor cells to become TAs (4). Recently, a role of Notch signaling in self-renewal was also proven in roundworms (21).

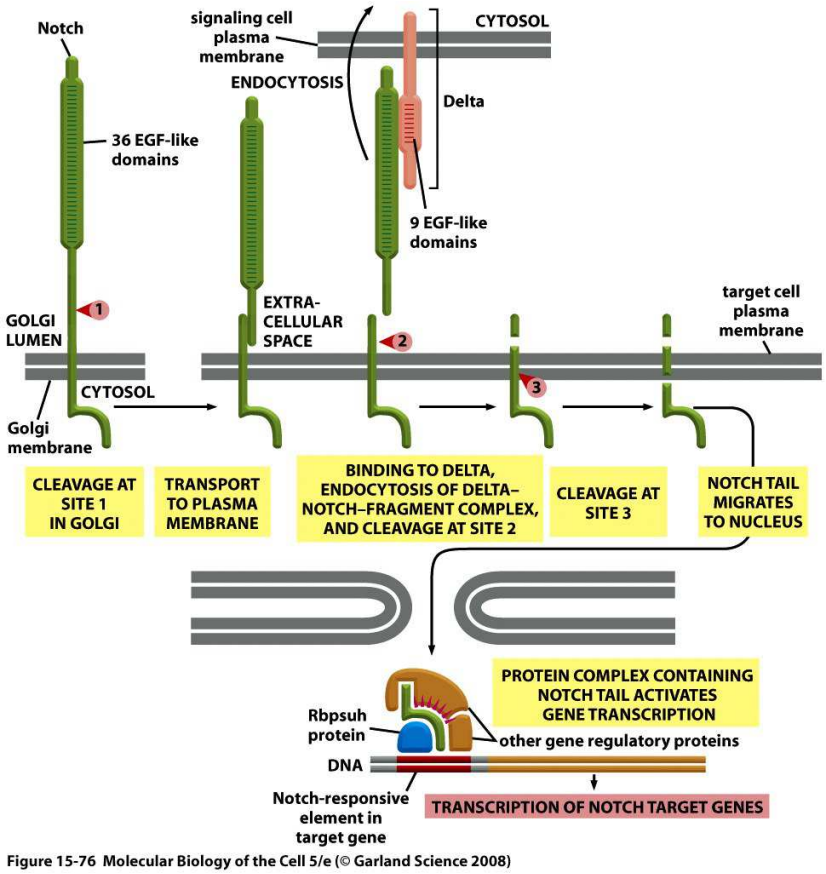

Figure 6: Notch signaling pathway. Source: ALBERTS B, JOHNSON A, LEWIS J et al. Molecular Biology of The Cell. Garland Science: New York, 2008; 1600.

1.1.6 Oral keratinocyte stem cells (OKSC)

Oral keratinocytes stem cells are, so far, difficult to purify. Nevertheless, several markers have been found to identify subpopulations with stem cell-like properties. And therefore are considered adequate only to enrich for keratinocyte stem cells.

$\alpha_6\beta_4$ integrin$^+$ CD71$^-$

Integrins are a family of transmembrane receptors that function as cell adhesion molecules. By binding to laminin-5 in the basement membrane, α6β4 integrin was found to be fundamental for hemidesmosome assembly, and its expression was found to be a characteristic of the basal layer keratinocytes in normal epithelium (22). Thus, it was theorized that α6β4 integrin can be used to isolate both the slow cycling stem cells and the rapidly proliferating early TAs. These observations were exploited to enrich for OKSCs, and cells positive for $\alpha_6\beta_4$ integrin but negative for the proliferation marker CD71 were found to display more stem cell properties as compared to $\alpha_6\beta_4$ integrin$^+$ CD71$^+$ cells (23).

CD44^{High}

CD44 is a transmembrane glycoprotein whose functions involve cell adhesion, motility, proliferation and survival (24). Normal human oral keratinocytes expressing high levels of CD44 were shown to display stem cell-like properties, including high proliferative capacity and resistance to apoptosis (25).

p75NTR

The low affinity nerve growth factor receptor p75NTR was found to identify clusters of slow cycling keratinocytes in the basal layer of oral epithelium (5). In vitro analysis of p75NTR+ oral keratinocytes indicated that this subpopulation is enriched in stem cells, and suggested a role of this molecule in maintaining cell survival (5, 26). P75NTR is a transmembrane receptor composed of extracellular, transmembrane and intracellular domains, and has been structurally affiliated to the tumor necrosis factor receptor superfamily (27). Depending of the type of cell and biological context,

p75NTR serves a wide spectrum of functions including survival, proliferation, apoptosis and differentiation. Functions of p75NTR was found to be modulated by its own level of expression, post-translational modifications, dimerization, ligand binding and engagement with co-receptors as well as intracellular partners (28). Interestingly, p75NTR was found to be expressed by mouse embryonic (29), mammalian neural crest (30, 31) and human esophageal keratinocyte (32) stem cells, in addition to several other extra neuronal stem/progenitor cells [reviewed by Tomellini *et. al* (28) and references therein].

1.1.7 Carcinogenesis and disruption of homeostasis

Carcinogenesis is a multistep process that results from accumulation of unrepaired DNA alterations that are passed on to the next generation of cells. Therefore, cancer is considered a genetic disease at the cell level (2). Over time, this may lead to genetic instability, and more mutations are likely to occur, including mutations in the tumor suppressor and/or proto-oncogenes (33). The accumulating mutations in a cell result in acquiring certain biological capabilities referred to as “the hallmarks of cancer” (34). Among others, cancer cells are capable of proliferating unlimitedly, and independently of exogenous growth signals. Moreover, they are capable of escaping growth inhibitory signals and destruction by the immune system and apoptosis (34). A logical consequence of such behavior is aberration of tissue homeostasis, and formation of a tissue mass whose growth exceeds that of a normal one, a tumor (33). Subsequently, there is a rising need, within a tumor, for oxygen and nutrients. Cancer cells evade this scarcity by inducing formation of new blood vessels (angiogenesis), and by local invasion and metastasis which are also among the hallmarks of cancer (34).

1.1.8 Oral Squamous Cell Carcinoma (OSCC)

In general, sites of oral cancer include the mucosae of the lips, cheeks, tongue, gingivae, palate and the floor of the mouth. In 2008, International Agency for Research on Cancer estimated 400000 new cases of oral and pharyngeal cancers per year (35). The incidence is highly variably in different geographical regions, and oral cancer was ranked as the sixth incident cancer in males in the developing

countries(35). In 2012, 300000 cases of oral cancer were reported worldwide (36). The most common type of oral cancer is OSCC, accounting for 90% of the cases (35, 37, 38). Risk factors of OSCC include, tobacco and alcohol use, infection with human papilloma virus or *Candida Albicans*, poor immunity, chronic irritation of the lip by exposure to UV light or the tongue by local friction with a sharp object (35, 39).

Like many other malignancies, OSCC is considered to be a multi-step disease, and progression from premalignant (dysplastic) lesions is a common finding (Figure 7). A major biological event in the progression of OSCC is metastasis to the regional lymph nodes (39). Routinely used treatment modalities are surgical resection of the primary tumor and cervical lymph nodes, radiotherapy and the combination of both, depending on the anatomic site and tumor stage (35, 39). Surgical resection often results in impairment of speech, nutrition and appearance depending on the extent of resection. Accordingly, health-related quality of life was found to be proportional to preoperative functional impairment caused by the tumor (40). Additional use of conventional chemotherapy yielded conflicting results, with the prognosis remaining poor in many reports (39, 41), and resistance developing during the course of the disease (41). Cetuximab, an antibody against epithelial growth factor receptor (EGFR), was found beneficial when given in combination with radiotherapy (42). Nevertheless, the survival rates remained virtually the same since 1980s, reflecting no major progress in the treatment (35, 43). Prognosis is influenced by the clinical stage and the histologic subtype. The overall survival rate for OSCC is below 50%, and occurrence of lymph nodes metastasis was found to result in a dramatic decrease in the survival rates, while early stage tumors were found to have a better survival rate (44). Histologic grading based on the differentiation level was found to be relevant to the patient prognosis and patients with highly differentiated tumors were reported to have better prognosis (39). Other prognostic indicators include, histological pattern of invasion (45), status of surgical margins (46), patient age, gender, general health and mental status (39). High rates of loco-regional recurrence of OSCC have been reported (47), and the poor survival rates and treatment failure have been attributed to that (48).

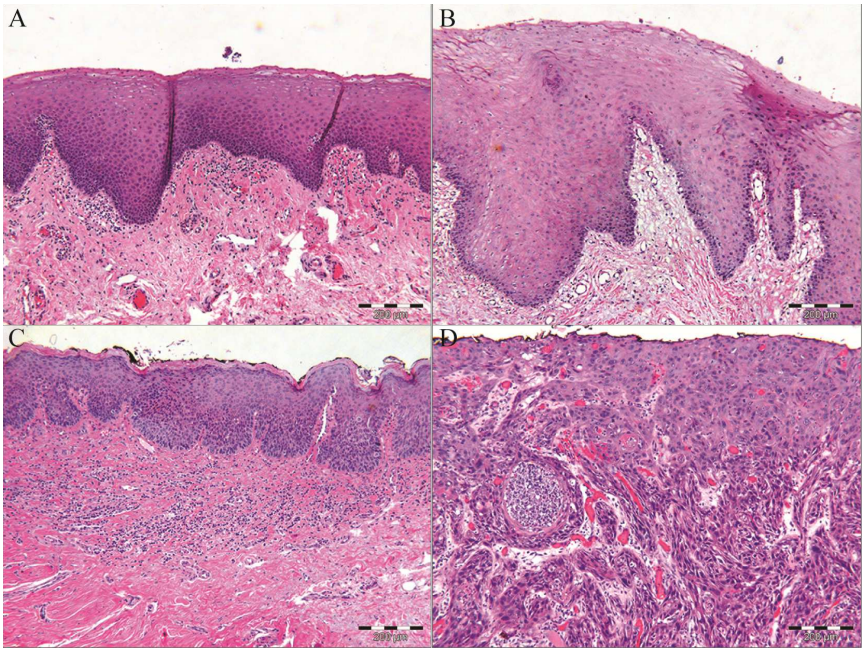

Figure 7: Hematoxylin and Eosin stained sections of: NHOM (A), Hyperplastic oral epithelium (B), Oral dysplasia (C), Invasive OSCC (D), own photos.

1.2 Heterogeneity of cancer

A cancer cell population is composed of genotypically, phenotypically and functionally different mixture of cells (2). New phenotypes that are resistant to cancer therapy are arising as the tumor grows, even with the use of some of the most successful molecular targeted modern drugs. The advancement in molecular biology has led to the discovery of a wide range of molecular targets for second generation drugs that can be used when resistance to the drugs in hand develops (2). The commencing discoveries in this field resulted in improvement of survival of patients with many types of cancer in Europe. However, the combined survival index of patients with all types of cancer is still below 50% and 60% for men and women respectively (43). Improving the survival rates, and the quality of life of cancer patients, require thorough understanding of the mechanisms involved in the heterogeneity of cancer cells.

Crosstalk between the tumor cells and their non-neoplastic surroundings was implicated in creating different niches within the tumor bulk, and amended neoplastic phenotypes that can better serve the progression of the disease are continuously emerging in response to the ever changing microenvironment (49). Nevertheless, the intrinsic mechanism by which the tumor cells give rise to tumor heterogeneity is still controversial, and models proposed are the clonal evolution model (33), the cancer stem cell model (2), and more recently, co-existence of the two models within the same tumor was suggested (50).

1.2.1 The clonal evolution (Stochastic) model

This model proposes that the first genetic changes in the carcinogenesis process are passed unrepaired from the parent cell to its entire progeny, which would further expand when the proliferation process gets out of control. Later on, further genetic changes would take place due to the genetic instability, resulting in further phenotypical differences that are inherited to the expanding generations of cells (33, 51). This model have been viewed as a Darwinian evolution, the cancer cells are obeying 'natural order', and the accumulating genetic changes would lead to adaptation to the microenvironment and selection of the fittest (2, 51). Tumor heterogeneity is, therefore, the result of the continuous stochastic emergence and expansion of new phenotypes that can better survive environmental changes.

1.2.2 The cancer stem cell (CSC) model

A cancer stem cell is defined as "a cell within a tumor that possesses the capacity to self-renew and to cause the heterogeneous lineages of cancer cells that comprise the tumor" (52). The role of stem cells in carcinogenesis was hypothesized during the 1800s, when the resemblance between teratocarcinomas and the developing fetus was thought to be due to activation of rudimentary embryonic rests (53). However, the technology available at that time was not sufficient to establish a compelling proof of these hypotheses. It was the 1990s when the cancer stem cell model was experimentally proven for acute myeloid leukemia (AML) (54, 55). This discovery has led to extensive research to investigate the existence and characteristics of CSCs in

many solid tumors such as breast (56), colon (57), brain (58) prostate (59), lung (60) , liver (61), and melanoma (62) .

This model proposes the existence of a small subpopulation of cancer cells possessing stem cell properties. This subpopulation is also referred to as the stem-like cancer cells (CSCs), the tumor initiating cells, or the tumorigenic cells (52). Comparable to tissue specific normal stem cells, this subpopulation is thought to be rare, enter the cell cycle infrequently, have the ability to self-renew, and to differentiate into heterogeneous phenotypes. Although the model does not address the cell of origin, it views a cancer cells population as an organ composed of a hierarchy of cells with different proliferation, differentiation, and more importantly, tumor initiation abilities. Accordingly, tumor heterogeneity is attributed to the continuing differentiation of CSCs through epigenetic modifications (52, 63, 64).

Origin of CSCs

The origin of CSCs is a controversial matter and several proposals have been adopted (65). In the first place, enrichment of CSCs in AML was based on the same markers used to enrich for normal hematopoietic stem cells (54, 55). This has led to the first proposal that leukemic stem cells result from transformed normal counterparts (53, 63). This proposal is supported by the postulation that the long life span of normal stem cells makes them more prone to accumulate mutations (2, 65). Nevertheless, consequent experimental work on AML revealed phenotypical differences between leukemic and normal hematopoietic stem cells (66). Experimental evidence has also showed that leukemic stem cells properties can be induced in hematopoietic progenitor cells only in some molecular subtypes of AML (67). Taken together, normal stem cells can be the origin of CSCs in some types of cancer (53).

Another suggestion is that self-renewal capacity could be acquired by a differentiating cell if the right pathways are switched on or off by the accumulated mutations (2, 65). Several molecular mechanisms were found to serve in maintaining a stable genome in the normal stem cells in some tissues (4, 68, 69), which renders this proposal more conceivable in those particular tissues.

Fusion of hematopoietic stem cell and a differentiated somatic cell, with the resultant cell being able to maintain self-renewal has been suggested to explain the origin of CSCs (65, 70). Yet another phenomenon referred to as neosis has also been described *in vitro* and suggested as possible origin of CSCs (71, 72). Neosis is based on the theory that DNA damage can lead to formation of senescent giant cells that can divide and give rise to stem like mononuclear cells known as Raju cells (71, 72). Giant cells have been identified in some carcinomas but they have been described as a secondary reactive event of the host rather than being of neoplastic origin (73, 74). Therefore, *in vivo* evidence of neosis is so far lacking.

CSC and invasion

For an epithelial tumor to metastasize, cell adhesion molecules has to be broken down which can make the cell disassemble and change its character. Moreover, they invade the connective tissue stroma and may metastasize to distant locations via blood and lymphatics (2, 39). Escaping from their normal compartment and break down of intercellular binding molecules, triggers a set of intracellular events that result in acquiring characters of the mesenchymal component. This process is a common event during embryogenesis and is referred to as epithelial to mesenchymal transition (EMT), and the origin of the neural crest during embryogenesis is one good example of it (4). Metastatic breast and colorectal cancers were found to contain CSCs (75, 76). In both tumors CSCs were found to have undergone EMT, and the resultant phenotype was given the name migrating cancer stem cells (13, 77). This phenotype retains stem cell properties, like quiescence ability, resistance to therapy and high proliferation potential, in addition to being more suited to invasion and metastasis.

CSCs and anti-cancer drug resistance

In addition to their role in tumor growth, heterogeneity and invasion, it has been theorized that CSCs can survive classical therapies designed to target highly proliferating cells, given their slow cycling rate at equilibrium (52) and indeed multiple drug resistance was shown for CSC and have been considered to be an intrinsic ability of these cells (50, 78, 79). The presence of membrane transporters as

ABCG2, can aid CSCs to efflux chemotherapeutic drugs (78). Moreover, resistance to new molecular targeted, comparatively successful, drugs like Imatinib was found to be a feature of leukemic stem cells (80, 81). It has also been reported that CSCs can survive ionizing radiation induced cell killing, by activation of DNA damage response (79), by having an extended G2 phase of the cell cycle which allows more efficient DNA repair (25), or by their high ability to scavenge reactive oxygen species (82). Based on these findings, it has been speculated that CSCs might be responsible of tumor recurrence after therapy.

The CSCs niche

Similar to their normal counterparts, CSC reside in specific niches within the tumor, that can regulate their self-renewal and differentiation abilities (83). Dynamic interaction between CSCs and their stromal partners has been reported in several cancers, and was found to contribute to the behavior of CSCs (84). In gliomas, CSCs were found to be chemoattracted to endothelial cells nearby to reside in a perivascular niche, and their tumorigenic ability was found to be enhanced by co-transplantation of endothelial cells (85). Perivascular CSC niche was also described at the invading front of OSCC, and co-culture with endothelial cells was shown to enhance survival and self-renewal of CSCs (86). In breast (87) and colon (88) cancers, CSC niche was observed at the invading front of the tumor, in close proximity to stromal cells that promote the invasion process.

Methods used for CSCs identification

Research in CSCs has inherited several functional methods that have been employed to identify normal stem cells. Firstly, long term retention of DNA analogues like, Bromodeoxyuridine, has been used to localize normal stem cells. This phenomena was first attributed to their slow cycling rate (89), and more recently to the observation that stem cells selectively segregate newly replicated DNA to the daughter cells (68). Nevertheless, employing the methods in a cancer investigation would underestimate the frequency of CSCs by missing the ones at a high proliferative state. Secondly, normal keratinocytes grown *in vitro* have been classified into stem cells, early and late

TAs according to their pattern of clonal expansion. In culture, the three subpopulations have been able to form holoclones, meroclones and paraclones respectively. Their ability to express certain molecules previously related to stemness, and to grow on further passages was found to be in accordance with the anticipated proliferative capabilities of the three cell types (90). Thirdly, sphere formation assay is based on the ability of stem cells to self-renew and differentiate independent of anchorage (91). Fourthly, differentiation ability of stem cells is investigated *in vivo* by transplantation into immunodeficient mice (9). When transplanted into immunodeficient mice, a CSC is presumed to recapitulate the heterogeneity of the original tumor it was derived from. Therefore, serial transplantation in animal models, also known as *in vivo* tumorigenicity assay, is regarded as the gold standard functional assay to identify a CSC subpopulation in a tumor (52).

Identification of distinctive markers for CSCs is considered a fundamental evidence for the existence of CSC in a particular tumor (64). Attempts to isolate CSC are often made by the use of fluorescent activated cell sorting (FACS) based on marker expression, prior to subjecting them to further functional assays (54, 55). The hunt for robust markers for CSCs in many tumors is still commencing, with the suggested ones resulting in a variable reproducibility and impurity (50, 52, 64, 92). Technically, the need to sort out viable cells has limited the selection of potential markers to the ones on the cell surface, like CD44, CD24(56) and CD133 (93). Exceptions of this are the isolation of cells according to their ability to expulse DNA binding dye Hoechst 33342 from their nucleus, and the activity of aldehyde dehydrogenases. Isolation of stem cells by flow cytometry as the side population (SP) that excludes Hoechst 33342 (94), is based on the expression of ATP Binding Cassette family (ABCs), which is a family of transmembrane proteins known to function as pumps to efflux toxic materials from inside the cell. Among other ABCs, the subgroup G2 (ABCG2 or BCRP1) is known to be expressed by stem cells (69). On the other hand, Aldehyde dehydrogenases (ALDH) are a family of intracellular detoxifying enzymes. There are at least 13 members of aldehyde dehydrogenases family in humans, classified into three classes. Their functions include detoxification of intracellular toxins, and metabolizing retinol during embryogenesis (95, 96). High activity of the isoform ALDH1A1 has been

suggested as a characteristic of both normal and cancer stem cells in the human colon (97) and breast (98), and has been suggested as a universal stem cell marker in many normal tissues and cancer types (99, 100). Aldehyde dehydrogenase-based cell detection assay has been developed and is commercially available as a kit [ALDEFLUOR^{TM}, STEMCELL technologies, Grenoble, France] (101, 102). This assay is based on a fluorescent, non-toxic substrate for ALDH1 that can diffuse freely into viable cells. In the presence of ALDH1, the utilized substrate is retained inside the cell, and the amount of fluorescent signal produced is proportional to the ALDH1 activity. This assay has been used for enrichment of normal and malignant hematopoietic stem cells (103, 104).

The CSCs phenotype in OSCC

As in many other solid tumors, the above mentioned methods have been employed for isolation of CSCs in OSCC, to further investigate their characteristic surface markers. Primary head and neck squamous cell carcinoma cells separated for CD44 expression and subsequent transplantation into NOD\SCID mice showed significantly higher tumorigenicity of CD44^{High} cells, as compared to CD44^{Low} cells (105). Tumors formed by CD44^{High} cells were found to recapitulate heterogeneity of the original tumors, with respect to histology and to the expression of CD44. Additionally, Immunohistochemistry (IHC) showed high expression of BMI1 in CD44+ cells. Although less incident, it is worth mentioning here that transplantation of CD44^{Low} cells at large numbers have resulted in tumor formation in the same study (105). This finding was attributed to low numbers of CSCs within CD44^{Low} subpopulation, and the authors reported CD44^{High} subpopulation to be enriched in CSCs. In subsequent studies, ALDEFLUOR^{TM} assay was found to identify a subpopulation of OSCC with CSC properties and CD44^{High} cells represented 50- 70% of that subpopulation (101). Transplantation into NOD\SCID mice revealed a tumor formation incidence of 24/25 and 3/37 for ALDH1^{br} and ALDH1^{di} OSCC cells respectively (106). Another study reported that ALDH1^{br} OSCC cells are undergoing EMT, and that knock down of Snail resulted in reducing their tumorigenicity (107). Enhanced radiosensitivity and decreased tumorigenicity of ALDH1^{br} OSCC cells by knock down of BMI1 was also

reported (108). In addition, $ALDH1^+$ cells were found to be present at the invading front of OSCC and that they co-express CD44 and matrix metalloproteinase -9 (106).

The dye exclusion method yielded a SP of OSCC that displayed higher colony formation, drug resistance and differentiation abilities *in vitro*, and tumorigenicity *in vivo*, as compared to non-SP (109, 110). Interestingly, SP of OSCC was also found to express higher levels of CD44 (105). Others investigators (111) focused on analyzing the spheres formed by OSCC cells, and found high expression levels of CD133, a putative CSC marker in brain cancer (58), that was previously found to be highly expressed by $CD44^{High}$ OSCC cells (112). Subpopulation of $CD133^+$ cells in OSCC was also found to display CSC properties and to be more resistant to chemotherapy (113). However, holoclones formed by OSCC cells, in another study, were found to exhibit weak CD133 by IHC (114), and *in vivo* tumorigenicity of CD133+ OSCC cells has not yet been tested.

1.2.3 Recent views on tumor heterogeneity

The latest perspective views heterogeneity of a population of cancer cells as a multifactorial process, in which clonal evolution, different microenvironmental conditions and cancer cell plasticity play a role in a tumor that might, or might not have a hierarchical organization (50). In the latter case, differences due to epigenetic modifications are only secondary to differences exerted by clonal evolution, and CSCs would arise stochastically from any of the neoplastic cells within a tumor (64). This prospective is supported by the failure, in some cancer types, to identify a pure CSC population and to reproduce or generalize the findings in other patients with the same tumor type (50, 64, 92). Findings from experimental work have also shown that CSC, in some tumors, may arise stochastically (76, 115, 116), and therefore, are considered a dynamic cell state rather than an individual cell type (117).

2. Rationale of the study

To date, none of the previously reported markers seem to specify a pure CSC subpopulation of OSCC cells. Expression of high ALDH1 levels was found to select a subpopulation of OSCC cells that exhibited stem cell behavior, and expressed high levels of CD44 (101). The same study found $ALDH1^{di}$ subpopulation to infrequently form tumors. This indicated that a more specific phenotypic signature is needed to isolate a pure CSC subpopulation from OSCC, and it was speculated that the combination of several markers might be necessary for yielding a pure CSC subpopulation (92).

Given the notion that CSCs may originate from their normal counterparts, the normal keratinocyte stem cell marker p75NTR comprises a putative CSC marker in OSCCs (5). High expression of p75NTR was found to correlate with poor prognosis in patients with OSCC (45). In esophageal squamous cell carcinoma, p75NTR was found to identify a self-renewing, chemotherapy resistant subpopulation (118), but it is not known if this is the case in OSCC or how this correlates with the ALDH1 activity.

In addition, recent reports have shown that the CSCs subpopulation is a rather dynamic compartment (115, 117, 119, 120). This have added more complexity to the model, and added variability over time as an additional factor (50). CSCs have been shown in OSCC to switch between two phenotypes, but the plasticity between non-CSC and CSCs in cancers in general and OSCC in particular is still a controversial issue and far from being elucidated.

3. Aims of the study

General aim

To investigate the pattern of expression of the normal oral keratinocyte stem cell marker p75NTR, and the CSC-related marker ALDH1A1, and their co-localization during OSCC progression from NHOM.

Specific aims

1- To establish a method for simultaneous immunohistochemical detection of several CSC-related markers (Paper I).

2- To identify the pattern of expression of p75NTR and ALDH1A1, relative to each other, during progression of OSCC from normal mucosa (Paper II).

3- To investigate the clinical significance of p75NTR, ALDH1A1 expression and their co-localization in OSCC patients (Paper II).

4- To investigate p75NTR as a putative CSC marker in OSCC (Paper III).

4. Methodological considerations

In the current work, a combination of both *in vitro* and *in vivo* experimental data and *in vivo* descriptive data from patient material was generated (Figure 8). Collection of samples and isolation of cells for use in this project were approved by the regional Medical Ethical Committee for West and North Norway. The use of *in vitro* assays has been criticized in some branches of the biomedical sciences (121). The method of isolation followed by grafting in foreign environment was found, for example, to induce changes in gene expression profile of beta cells isolated from pancreas (122, 123), and fundamental behavioral changes were considered a cell culture artifact (124). Although provided with the basic nutrients and growth factors, monolayer submerged cultures lack the dynamic conditions, the interaction with other types of cells and the tissue architecture found *in vivo* (125-128). However, *in vitro* assays have major advantages compared to *in vivo* assays in addition to being more feasible and less technically and financially demanding, like the wide array of commercially available kits and reagents, as well as the flexibility conferred to carry out various experimental designs to answer specific hypothesis. Therefore, the use of *in vitro* stem cell assays is advocated given certain conditions (52). Careful discussion and interpretation of our data indicated consistency between the two types of methods for the key findings of the present study.

Details of the methods employed are described in the respective papers attached to this thesis. Briefly, a protocol for triple IHC was established (Paper I), and expression of p75NTR and ALDH1A1, and their co-localization with BMI1 (CSC-related markers) was investigated in NHOM, OD and OSCC formalin fixed paraffin embedded samples (whole OSCC biopsies and tumor cores constructed in TMA) (Paper II) by use of the method developed in paper I. Frequency of positive cells and co-localization of the three CSC-related markers was scored semi-quantitatively, dichotomized, compared between the three types of samples, and investigated for clinical significance in OSCC patients. Subsequently, anti-BMI1 antibody was replaced by anti-Ki67 antibody in a similar triple IHC protocol. Percentage of Ki-67 positive cells within $p75NTR^+$, $ALDH1A1^+$ and $p75NTR^+ALDH1A1^+$ was determined and compared to each other, as

well as across the three types of samples (Figure 8A). Comparison between the expression levels of CSC-related markers was also compared between the tumor center and invading front, using triple IHC as well as qRT-PCR in laser microdissected pieces from FFPE OSCC samples (Figure 8A).

To investigate the expression of CSC-related markers in OSCC derived cell lines (Paper II), a panel of cell lines derived from NHOM, OD and OSCC were grown in the appropriate type of medium under standard culture conditions. Cells were simultaneously investigated by FACS for ALDH1 activity using ALDEFLUOR^{TM} assay, p75NTR expression using a two-layered immunostaining and CD44 using a directly conjugated antibody (Figure 8B). Although ALDEFLUOR assay employs a specific inhibitor to ALDH1A1 as a negative control, the substrate was found to react to other isoforms of ALDH1 (129). Therefore, cells sorted using this method will be referred to, throughout the thesis, as ALDH1$^{br/di}$ for bright and dim respectively.

To investigate the stem cell properties of p75NTR^{High} cells (Paper III), p75NTR^{High} and p75NTR^{Low} CaLH3 cells were sorted out using FACS, and collected in FAD medium. Both subpopulations were used for *in vivo* and *in vitro* stem cell assays, cell cycle analysis, drug resistance and quantitative RT-PCR (Figure 8B).

To investigate the change in expression of p75NTR and ALDH1 over time (Paper II & III), the sorted subpopulations were propagated in culture for a week, and the FACS analysis was performed once more. Xenografts formed by injection of the two subpopulations were subjected to immunohistochemistry for p75NTR, Ki-67 and involucrin (Figure 8B, green arrows).

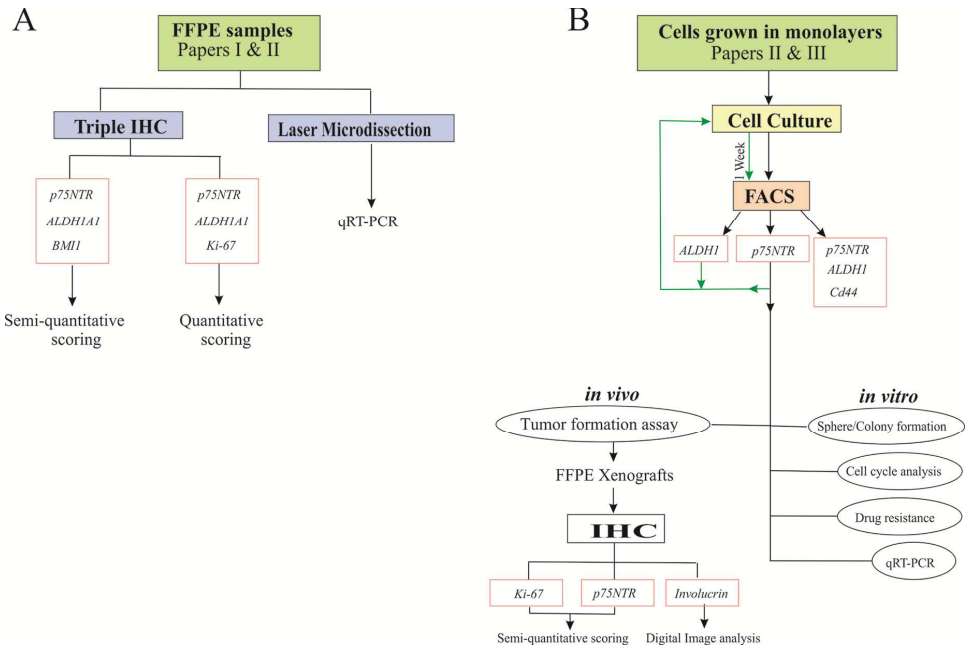

Figure 8: Flow chart of the methods used in the project.

4.1 The use of formalin fixed archival tissues (Paper I & II)

Fixation of tissues in cross-linking fixatives involves structural changes in the tissue proteins, and may have adverse effects on subsequent immunohistochemical reactions (130-132). The samples used in this study where archival formalin fixed/paraffin embedded tissues, with no available information about the duration of fixation (Paper I & II). To control for false negative samples, an internal positive control have been employed for each of the targeted antigens. These were lymphocytes for BMI1 and ALDH1A1, and nerve tissues for p75NTR. Repeated lack of a detectable immunoreactivity of any of the internal controls would result in exclusion of the sample from further analysis (Figure 9). To control for unspecific binding, one tissue section was assigned as a negative control, in which incubation with primary antibody was omitted and a non-binding negative control mouse IgG1 (DAKO, Golstrup, Denmark) was used instead. Additionally, endogenous enzyme activity was quenched

using the appropriate substrate, and blocking with normal serum equivalent to the secondary antibody was performed on every experiment.

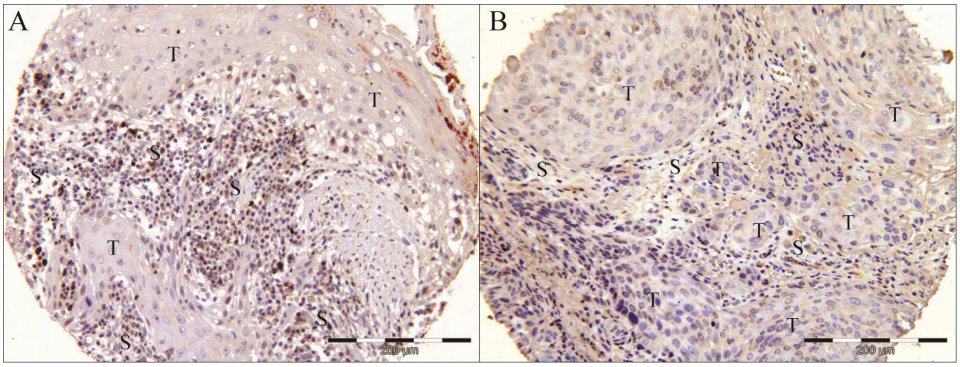

Figure 9: FFPE samples from OSCC immunostained for BMI1 (brown nuclear color). Immunoreactivity observed both in the tumor cells and the tumor stroma (lymphocytes and fibroblasts) (A). Lack of distinct reaction in the stroma (B) resulted in exclusion of the sample.

4.2 The choice of primary antibodies and triple IHC (Paper I & II)

The anti-ALDH1A1 antibody used for IHC in this project (BD Biosciences, New Jeresy, USA, 1:250) was previously found to identify a subpopulation of ALDEFLUOR positive cells and none of the ALDEFLUOR negative cells (98). The choice of anti-BMI1 antibody was also based on previous publications [Merk Millipore, Massachusetts, USA (12, 109, 133, 134)]. For optimization of the IHC protocol, samples from human testis and cervical lymph nodes were used as positive controls, and the two antibodies were tested individually (135). In our hands, anti-BMI1 antibody was found to show a specific IHC nuclear reaction with good intensity when epitope retrieval was performed by heating the sections to 125℃ in Target Retrieval Buffer (pH 6.0, Dako), using a pressure cooker (Decloaking Chamber^{TM} , Biocare Medical, California, USA). The adequate dilution range for each of the two antibodies was determined accordingly. The anti-p75NTR antibody (Sigma-Aldrich, St. Louis, USA) (136), used for both FACS and IHC in paper III, gave the best signal

to noise ratio by performing enzyme induced epitope retrieval as recommended by the manufacturer. To overcome this problem in our proposed triple staining, another monoclonal mouse anti-p75NTR antibody (Millipore) (5, 118, 137), that works with the same retrieval method as the other two antibodies was tested and subsequently adopted for triple IHC. In addition, mouse monoclonal anti-Ki67 (Dako) was included in the investigation.

Based on these choices, the next challenge was to combine three unconjugated mouse antibodies from the subclass IgG1 in a triple IHC protocol. Triple staining was conducted sequentially, and the reactions were detected using the following methods: i) labeled polymer-horseradish peroxidase conjugated to goat anti-mouse immunoglobulins (LP-HRP, EnVision+ ®, Dako). ii) Mixture of biotinylated goat anti-mouse and anti-rabbit immunoglobulins (REAL LINK ®, Dako), followed by streptavidin conjugated to horseradish peroxidase (REAL Streptavidin Peroxidase®, Dako). iii) Dextran polymer coupled with secondary antibodies against mouse and rabbit immunoglobulins (Link rabbit/mouse®, Dako), followed by labeled polymer-alkaline phosphatse anti-mouse/rabbit (LP-AP, Dako). Incubation with secondary immunoreagents was performed according to manufacturer`s instructions. Chromogens used were 3,3`-diaminobenzidine tetrahydrochloride (DAB), Permanent Red (both from Dako), ImmPACT SG and ImmPACT VIP (both from Vectorlabs, California, USA), resulting in grey, purple and red colors respectively.

Different approaches were tested to prevent cross-reactivity between subsequent reactions. Firstly, the shielding effect of DAB was investigated using different dilutions for the respective primary antibody as reported before (138). Secondly, a commercially available blocking solution that is a part of the *EnVision ™ G|2 Doublestain* System (Dako), was tested for triple staining, with or without a saturation step using a non-binding Negative Control Mouse IgG1 (139). Thirdly, the use of microwave heating for denaturation of antibodies from preceding reaction was also investigated as previously reported (140, 141). The order of the reactions and chromogens assigned to them was based on the antigens subcellular localization, the resulting signal intensity, shielding effect of the chromogens and their ability to

withstand denaturation steps. The experiments were performed as illustrated in Figure 10.

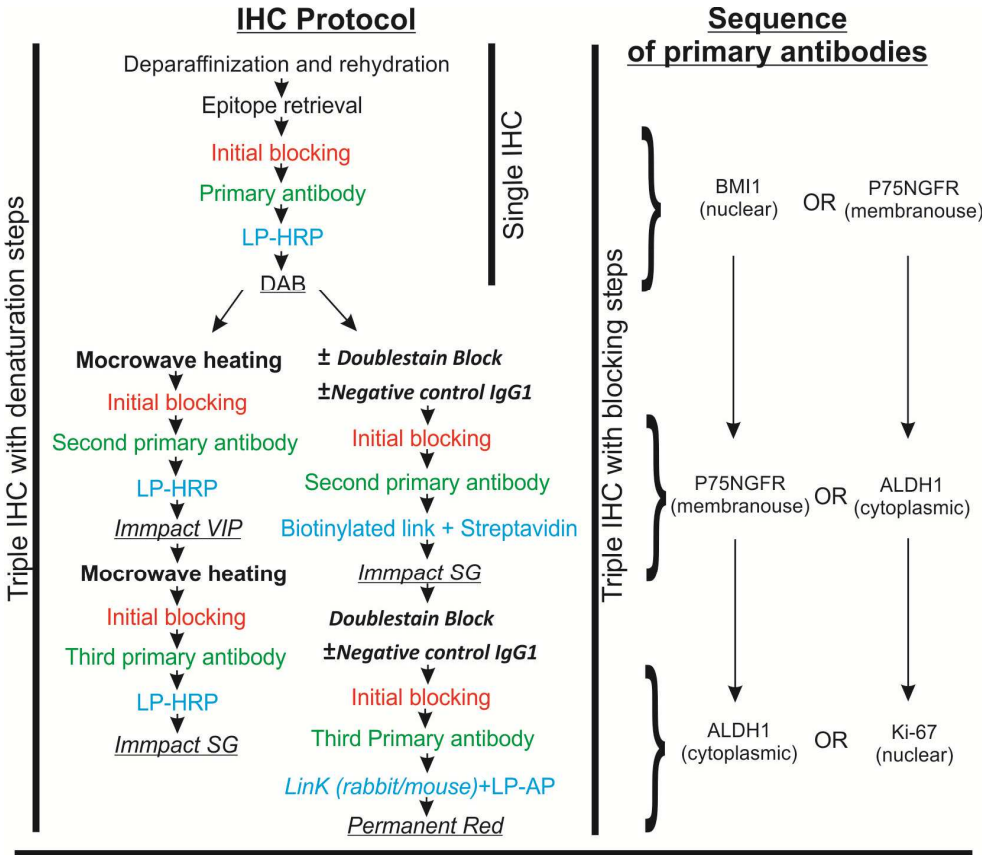

Figure 10: Flow chart illustrating the IHC protocol and the sequence of primary antibodies (Source: Paper I).

4.3 Evaluation of IHC, visual *vs.* digital (Paper I, II & III)

Visual evaluation of the immunostaining was performed by one observer after calibration of IHC scores with two co-workers. The scoring systems employed were based on the literature (Table 1), and calibration was performed on triple stained sections. For patient material (Paper II), the observer had no prior knowledge of the clinical information of the patients. For the xenografts (Paper III), the slide labels were covered until the evaluation process is finished.

score	BMI1(142)	p75NTR (143)	ALDH1A1 (144)
0	<1 %	<1 %	<5 %
1	1-25 %	1-25 %	5-25 %
2	26-50 %	26-50 %	25-50 %
3	>50 %	>50 %	>50 %

Table 1: Semi-quantitative IHC scoring of CSC-related markers.

Digital image analysis is commonly used for immunofluorescence, and only rarely for bright field microscopy (145). Visual evaluation of tissue sections subjected to multiple immunoenzyme staining requires careful selection of chromogens, and the color products have to be well contrasting to the human eye (131, 145). The task is more challenging when co-localization of the reactions products is of interest, then the mixture of the chromogens at the site of co-localization should have a distinct color (131, 145). Nowadays, several systems for evaluation of immunoenzymatically stained slides are available, the technologies used by different systems were reviewed by Mulrane *et al* (146). In this project, ScanScope ® system was employed in paper I to validate the usefulness of the combination of colors used. While in paper III, the method was used to compare the intensity of involucrin staining between the two xenografts groups (Figure 11).

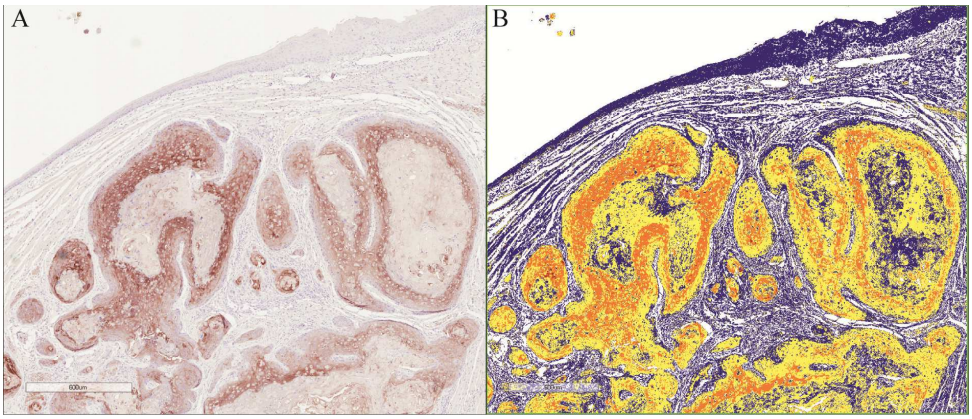

Figure 11: Xenograft model stained for Involucrin (brown)(A), the markup image generated by the color deconvolution algorithm, intensity of the staining is reflected by yellow to red color, blue represents negative structures (B).

4.4 Cell lines and culture conditions (Paper II & III)

A panel of cell lines was used in this study. Oral squamous cell carcinoma derived cell lines: CaLH3, 5PT, Neo (known as PE-CA/PJ15) (147), primary OSCC cells LuC4 (148), and oral dysplasia derived cell lines: DOK, Poe9n (149) and D20 (150). Normal keratinocytes were isolated from gingival NHOM donated by four patients undergoing wisdom tooth extraction at Haukeland University Hospital after informed consent. All OSCC cell lines and primary cells were grown in DMEM medium supplemented with 25% nutrient mixture F-12 Ham, 50 µg/ml L ascorbic acid, 0.4 µg/ml hydrocortisone, 10 ng/ml epithelial growth factor (all from Sigma-Aldrich, St. Louis, MO, USA), 10% fetal bovine serum (FBS) and 5 µg/ml insulin (both from Life technologies, CA, USA), also known as FAD medium (126).while normal keratinocytes and Poen9 were grown in Keratinocytes serum free medium (KSFM), supplemented with 10 ng/ml epithelial growth factor and 25 µg/mL bovine pituitary extract (Life technologies). All cells were grown under standard culture conditions.

4.5 FACS analysis and controls (Paper I & III)

All FACS procedures were performed in BD FACSAriaTM IIu (BD Biosciences, NJ, USA). Separation of cells for p75NTR (1:250, Sigma) expression was based on the threshold detected by incubating part of the sample with a negative control mouse IgG1(Dako) instead of the primary antibody. Secondary antibody used was Alexa Fluor® 488 F(ab^{1})2 fragment of goat anti-mouse H+L (1:250, Life technologies), and emitted fluorescent signal was read using 525/50 BP filter.

Similar approach was followed when cells were separated for ALDH1 activity using ALDEFLUOR^{TM} assay. Part of the sample was incubated with DEBAB to inhibit ALDH1 activity, according to the manufacturer`s instructions. Postsort checking was performed after each of the sorting sessions. The error detected by post-sort check comprised 1-2%, and may be attributed to loss of the fluorescent signal of the secondary antibody, or effluxing the ALDEFLUOR reagent from inside the cells during the FACS procedure. In general, the purity of the sorted subpopulations seemed to be related to the length of the sorting session.

Same negative controls were employed for detecting the frequency and overlap between p75NTR, ALDH1 and CD44 subpopulations simultaneously. In those experiments, secondary antibody used to detect p75NTR reaction was conjugated to AF 647, which has a different emission wave length from ALDEFLUOR^{TM}, while CD44 was detected using PE-mouse antihuman CD44 (BD biosciences 1:1000). This has enabled reading the emitted signals through different filters as illustrated in figure 12.

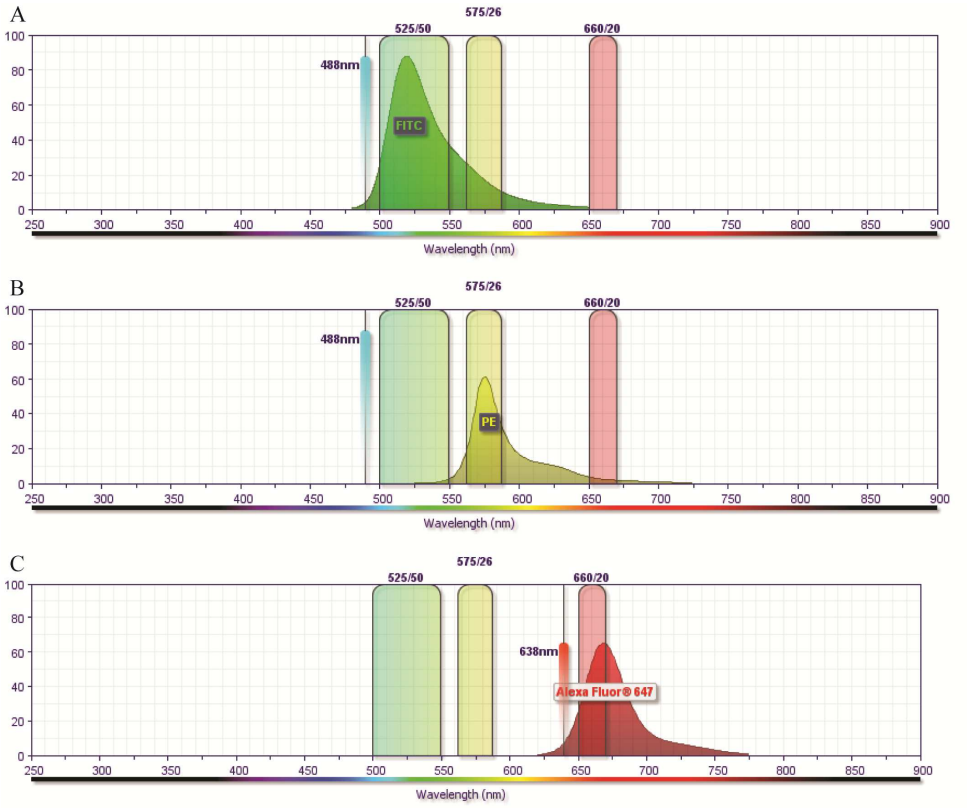

Figure 11 : Illustration of the difference in excitation, emission and filters used for ALDEFLUOR™ assay (A), PE (B) and AlexaFluor® 647 (C). Source: BD spectrum viewer (http://www.bdbiosciences.com/research/multicolor/spectrum_viewer/)

4.6 The choice of the animal model (Paper III)

The animal experiments were approved by the Norwegian Animal Research Authority, transplantation of the tumor cells was conducted under anesthesia (Figure 13), and none of the mice needed to be euthanized before the end of the experiment.

It is considered that *in vivo* tumorigenicity assay must be performed in the most possible permissive conditions, so as to avoid underestimation of the cells with a tumor formation potential (50). Adhesion molecules and growth factors essential for the growth of the transplanted human cells might not be available in the new microenvironment (151, 152). In this project, transplantation of cells was done

orthotopically, the OSCC cells being injected into the tongue of mice. The advantage of this was reported to mimic the original microenvironment of the OSCC cells, offering a more normalized conditions than in other sites (153). Additionally, cells were suspended in reduced growth factors *Matrigel* (BDbiosciences) to provide them with a matrix that would help for tumor growth.

The effect of the animal`s immunity on the transplanted human cells would also hinder determination of all the tumorigenic cells evident (154, 155). The animal model used in this project was NOD\SCID IL2Rɤnull mice, also known as NSG, which lacks natural killer cells, T and B-cells and have defective macrophages and dendritic cells (156). Being one of the most immunodeficient available strains, NSG mice comprise a relatively permissive environment as compared to NOD\SCID mice that have retained their natural killer cell activity (50, 157). It was reported that unselected melanoma cells are more likely to form tumors in NSG mice compared to NOD/SCID (116). On the other hand, a role of macrophages in promoting invasion of gastric cancer cells was shown (158). In that senesce, the model might be less permissive for studying metastasis. Ideally, generation of immunocompetent autochthonous models for human OSCC would comprise a better model (155, 157).

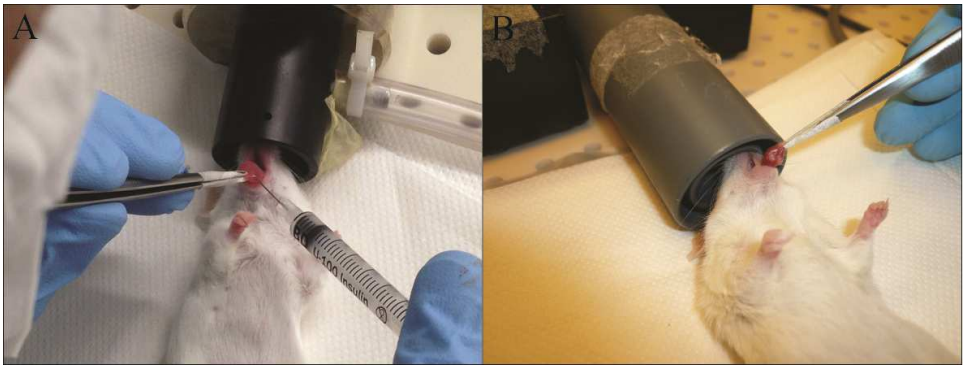

Figure 13: Transplantation of OSCC-derived cells into the tongue of the mouse under anaesthesia (A). Appearance of the tumor, weeks later, on the inferior surface of the tongue (B)

4.7 Laser microdissection of FFPE OSCCs

Sections of 15 micron thickness of FFPE OSCCs were placed on membrane coated glass slides (MembraneSlide NF 1.0 PEN, Zeiss, Oberkochen, Germany), after activating the membrane with UV light for 30 minutes. Slides were then incubated at 56 °C for 2 hours, de-paraffinized in xylene for 4 minutes, rehydrated in graded ethanol, stained with methylene green (Dako), and dehydrated in reverse graded ethanol and xylene. Fifty to hundred μm^2 tissue specimens from the tumor center and the corresponding invading front of each OSCC sample were laser microdissected (Figure 14) using a Zeiss Axiovert 200 inverted microscope equipped with a microlaser system (P.A.L.M Microlaser Technologies). Microdissected tissues were collected in nuclease free tubes (AdhesiveCap, Zeiss) and subjected to RNA extraction using RNeasy FFPE Kit (Qiagen, Limburg, Netherlands).

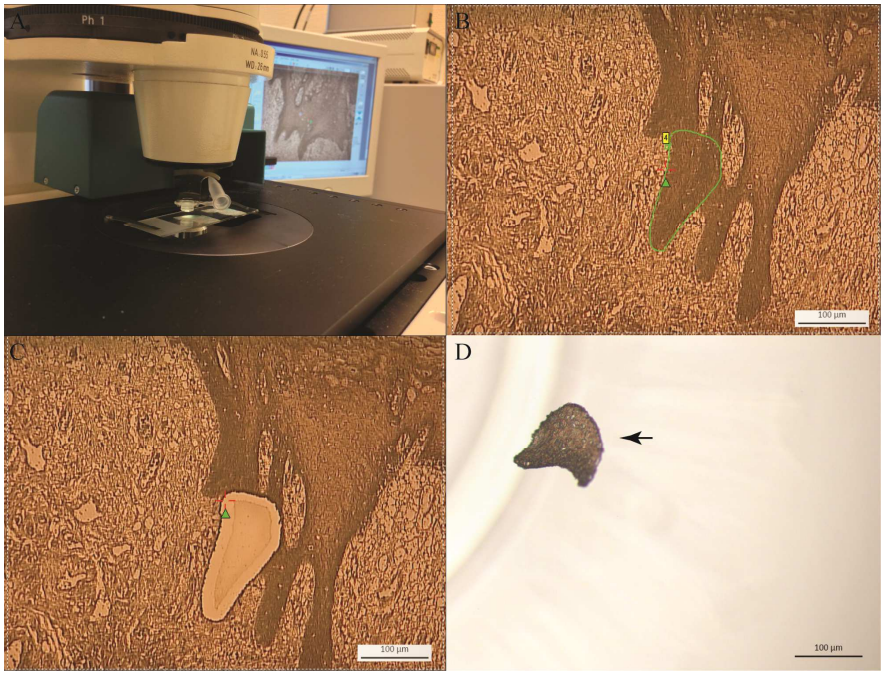

Figure 14 : P.A.L.M microlaser equipment with membrane slide and adhesive cap in place (A), screen shots of the area selected for microdissection (green line) (B), and after microdissecting and catapulting the selected area (C). The catapulted piece in the adhesive cap as photographed under the light microscope (black arrow) (D).

4.8 Statistical analysis

Analysis of qRT-PCR data (Paper II & III) was performed in *GraphPad Prism 6* (GraphPad, CA, USA), while all other statistical procedures were conducted in *Statistical Package for Social Sciences* (SPSS), version 19 (IBM, NY, USA). Immunohistochemistry scores have been dichotomized and dealt with as a categorical variables, correlation to clinical parameters was therefore investigated using Chi-Square test and fissure exact test as appropriate. Comparison of IHC scores between different areas of the same sample was performed by using McNemar test. For continuous variables, the choice of parametric Vs non-parametric statistical tests was based on exploring the normality of the distributions using Shapiro-Wilk`s test. Survival analysis was performed using Kaplan-Meier`s analysis, and possible confounding factors were investigated using Cox proportional hazard models. The level of significance was set to 0.05, results are presented as (mean ± SD) for continuous variables and statistical tests used are mentioned in their respective parts in the thesis.

5. Results

5.1 Successful triple IHC protocol for simultaneous detection of CSC-related markers (Paper I)

Consistent with a previous report (145), shielding effect of DAB was found to be dependent on the dilution of the respective primary antibodies. In our experiments, high dilution of primary antibodies whose reactions were visualized with DAB resulted in a mixed color when subsequent reaction was performed directly afterwards, while low dilutions resulted in less immunoreactivity of neighboring antigens (picture not shown). Sections subjected to triple IHC by employing a blocking step showed cross reactivity, and spurious color was evident despite the use of different detection systems (Figure 15).

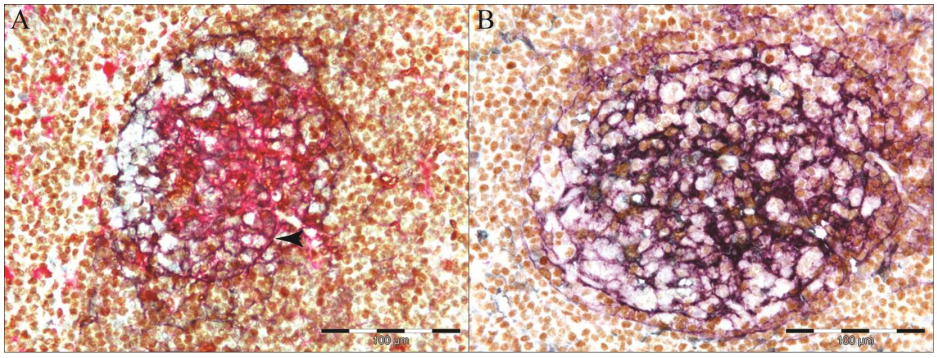

Figure 15: Section from FFPE sample of cervical lymph node subjected to triple IHC protocol employing a blocking step, BMI1 (brown), p75NTR (purple), ALDH1A1 (red), arrow head indicates a mixed color at the cell membrane (A). Similar section subjected to triple IHC protocol employing a denaturation step, BMI1 (brown), p75NTR (purple), ALDH1A1 (gray), no cross reaction observed.

Comparing sections subjected to triple IHC protocol employing a denaturation step to the ones subjected to single staining, showed a consistent staining pattern for each of the reactions. Furthermore, specificity of each of the three reactions was evident when

negative control mouse IgG was used to replace one of the primary antibodies at a time (Figure 16). The three reactions were found consistent with the expected types of cells and the subcellular compartment, despite the use of the same secondary immunoreagent for all reactions.

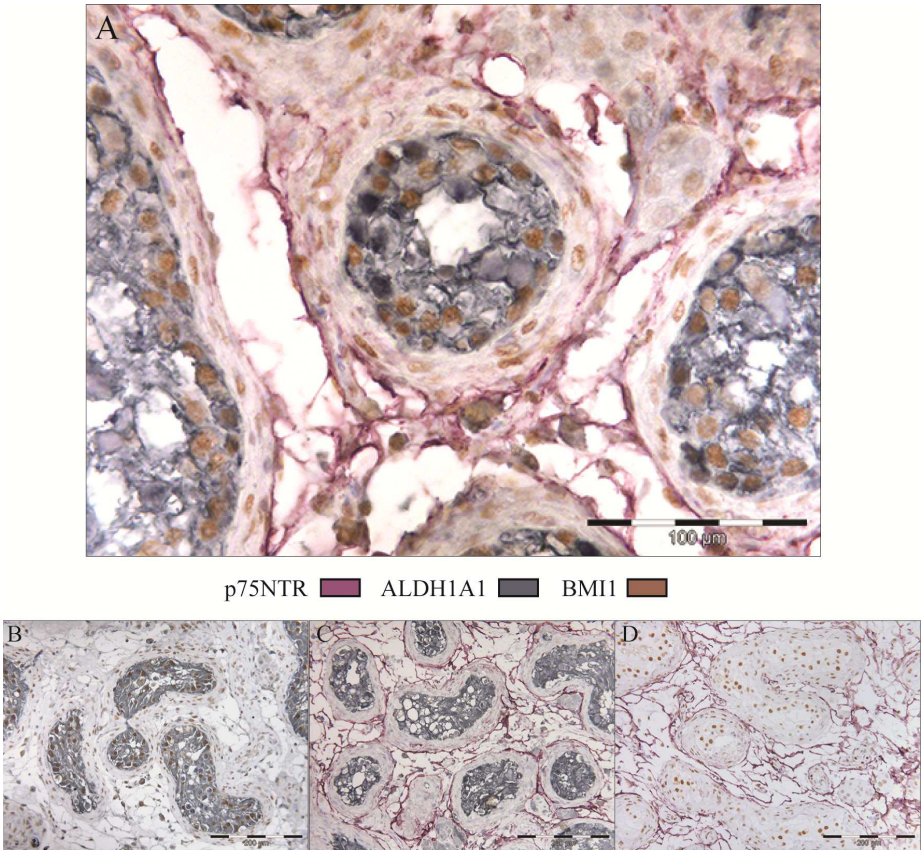

Figure 16: sample from human testis subjected for triple IHC with denaturation steps, BMI1 (brown), p75NTR (purple), ALDH1A1 (gray) (A),sections from same sample subjected to the same IHC protocol, but one of the antibodies was replaced with a non-binding mouse IgG1 (B-D).

The colors produced by the three reactions were found distinguishable even in cells where the three antigens were co-expressed, as evident by digital image analysis (Figure 17). These data show that the denaturation IHC protocol reported here is reliable for simultaneous detection of three antigens located in different subcellular compartments.

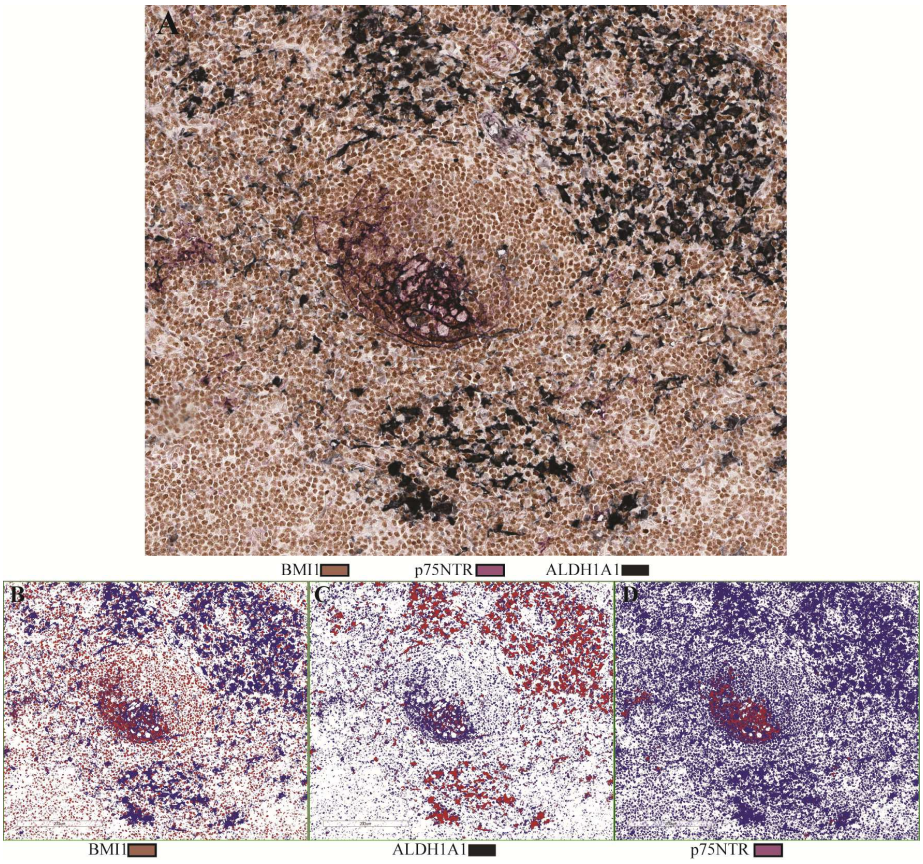

Figure 17:Human cervical lymph node sample subjected to triple IHC protocol involving denaturation steps (A). Markup images for each of the reactions as generated by the algorithm (B-D).

5.2 Triple IHC revealed higher frequency and wider distribution of the expression of CSC-related markers in OSCC and OD compared to normal mucosa (Paper II)

5.2.1 Simultaneous expression of CSC-related markers by cells of the basal layer in NHOM

Triple IHC identified the three CSC-related markers in 23 (74.2 %) of the NHOM samples included in the study. Eight (25.8 %) samples were found to be negative for ALDH1A1.

Expression of p7NTR was identified as a membranous staining of groups of the basal layer cells, at the tips of both the rete ridges and the connective tissue papillae (Figure 18). Accordingly, the percentage of $p75NTR^{+}$ cells was found to be consistently low, but present in all NHOM samples (Figure 19A).

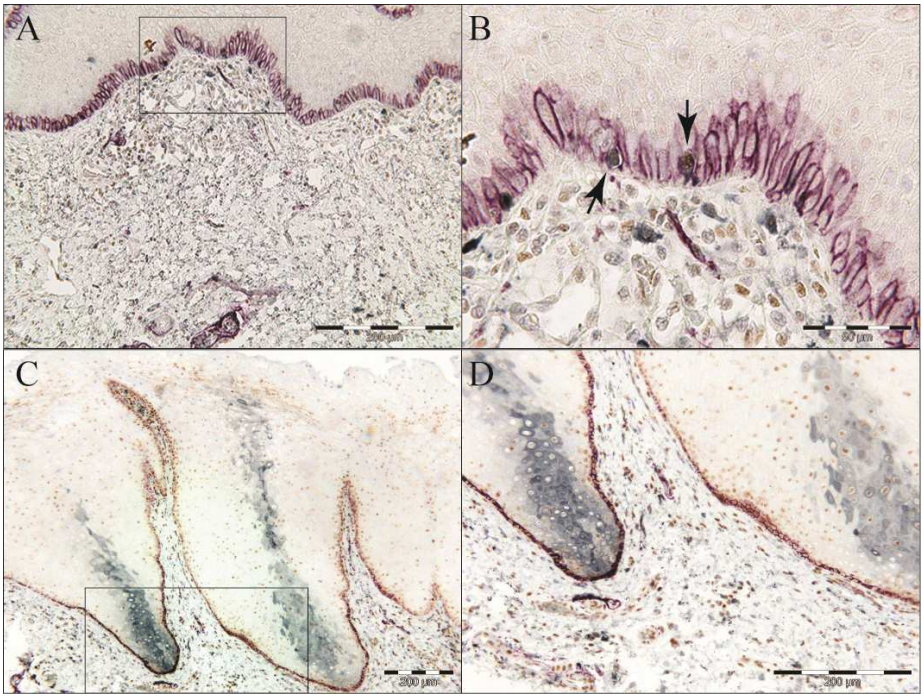

Figure 18: Representative example of NHOM subjected to triple IHC for CSC-related markers, BMI1 (brown), p75NTR (purple), ALDH1A1 (grey). Triple positive cells detected within the basal layer (A,B arrows). ALDH1A1 positive cells distributed in vertical patches (C,D)

Immunoreactivity for ALDH1A1 was detected as cytoplasmic with or without nuclear staining. Most of NHOM samples (67.7%, N= 21) scored 0-5% ALDH1A1$^+$ cells (Figure 18A,B). Keratinocytes positive for ALDH1A1 were located at both the basal and spinous cell layers. A particular distribution of ALDH1A1$^+$ cells was found in the two samples scoring 25-50% ALDH1A1$^+$, involving vertical patches /clones of keratinocytes from the basal layer till superficial layers (Figure 18C,D, Figure 19B).

Nuclear staining for BMI1 was detected both in the basal and spinous layers of the epithelium in all NHOM samples (Figure 18), and high frequency of positive cells (>50%) was detected in 8 samples (25.8%) (Figure 19C).

The overlap between p75NTR+ and BMI1+ cell populations was evident within the basal layer cells in all 31 samples. Rare cells co-expressing the three CSC-related markers were found in the basal layer compartment of 20 samples (64.5 %).

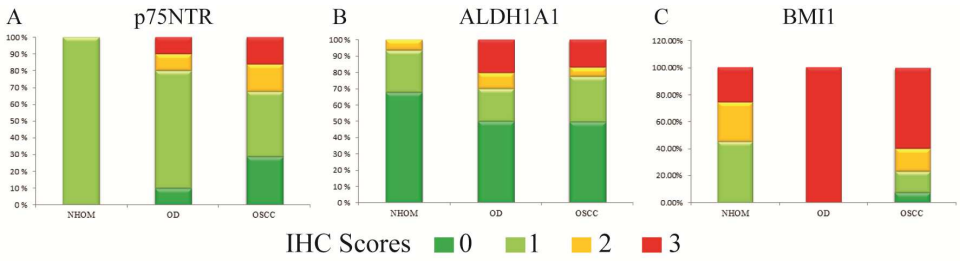

Figure 19: Scores of IHC for p75NTR (A), ALDH1A1 (B) and BMI1 (C) in the three types of samples.

5.2.2 Increased scatterness of the frequencies of the three cell populations in OD compared with NHOM

70% of the OD samples had low frequency of p75NTR positive cells (Figure 19A). Expression of p75NTR by 25-50% of the cells was detected in two samples, including some of spinous cell layer cells. One sample showed no p75NTR$^+$ cells, despite the immunoreactivity of the nerve tissues in the section. The same observation was made for ALDH1A1, and >50% positive cells were detected in two samples (Figure 20E),

and no ALDH1A1 cells were detected in two others (Figure 19B). In all 10 OD samples, BMI1+ cells comprised more than 50% of the epithelial cells in the section.

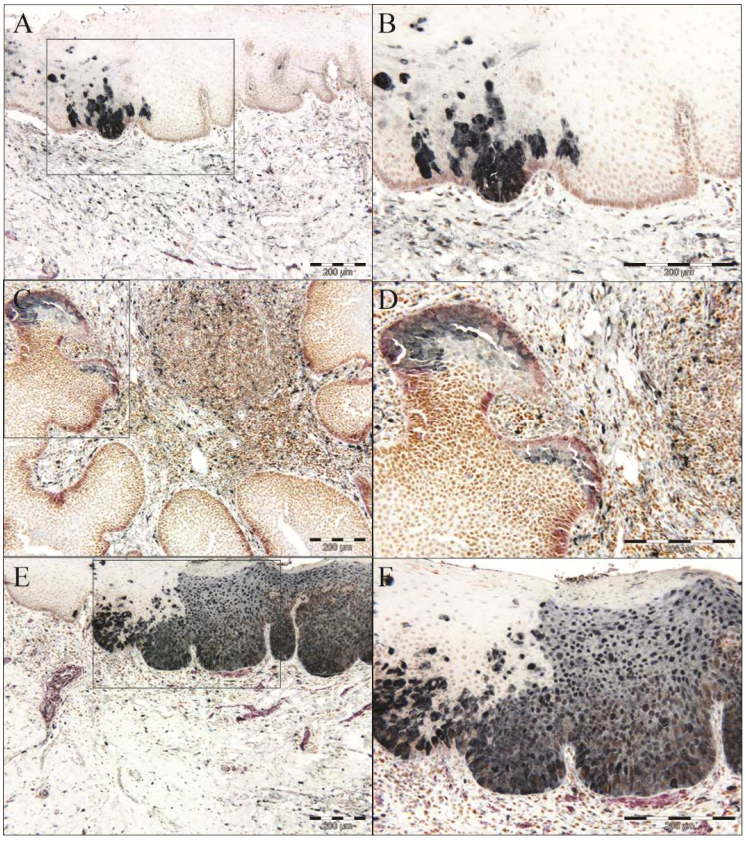

Figure 20:Representative examples of ODs stained for CSC related markers (A-F), BMI1 (brown), p75NTR (purple), ALDH1A1 (gray).

A statistically significant increase in the number of cells positive for each of the CSC-related markers was found in ODs as compared to NHOMs (Chi-Square test, Figure 21).

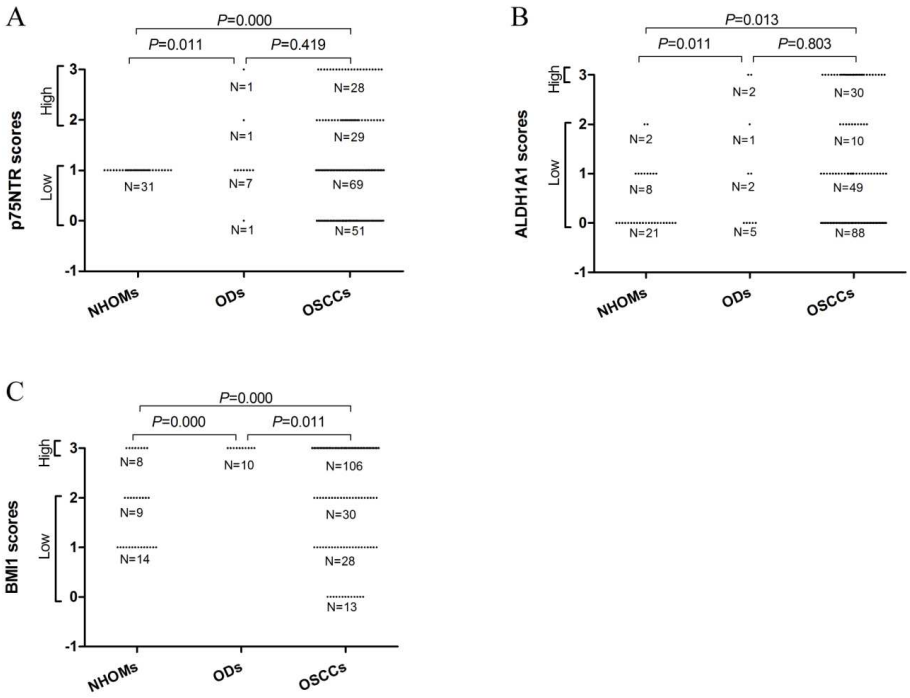

Figure 21:Scatter plots showing comparison of the dichotomized IHC scores for p75NTR (A), ALDH1A1 (B) and BMI1 (C), between the three types of samples.

In addition, the clone like distribution of ALDH1A1^{+} cells was more frequently detected (30%) among OD samples (Figure 20A,B). Co-localization of p75NTR or ALDH1A1 with BMI1 was detected in all samples expressing the two markers (n= 8 and 9 respectively). However, half of the OD samples were lacking the overlap of p75NTR^{+} and ALDH1A1^{+} populations (Figure 22).

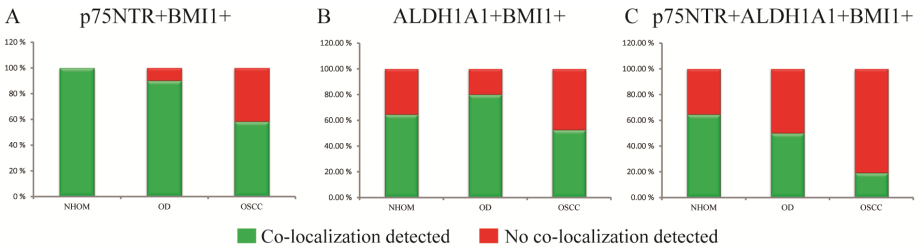

Figure 22: Detection of co-localization of CSC-related markers in the three types of samples.

5.2.3 Higher and increased heterogeneity in the expression of CSC-related markers in OSCC compared to NHOM and OD

Triple IHC revealed that 15.8% (n= 28) of OSCC samples expressed p75NTR by >50% of the tumor cells, with p75NTR+ cells detected in multiple layers (Figure 23). On the other hand, 28.8% (n= 51) had <1% p75NTR^{+} cells. Expression of ALDH1A1 by >50% of the cells was detected in 16.9% (n=30) of OSCC samples (Figure 19). Cells positive for ALDH1A1^{+} were detected both at the peripheries of the invading islands, and at the more differentiated central areas (Figure 23). Expression of BMI1 was also variable, with 59.9% (n=106) of the samples scoring three, and 7.3% (n=10) scoring 0. For all of the three CSC-related markers, disparity of the expression was observed even between different areas within the same OSCC sample (Figure 23).

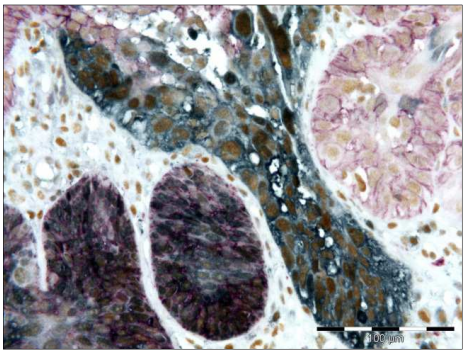

Figure 23: Representative example of an OSCC sample stained for CSC-related markers, same colors as figure 18.

With the exception of BMI1, statistical significance was achieved when the dichotomized IHC scores for CSC-related samples in OSCC were compared to NHOM (Chi-Square), but not when compared to ODs (Figure 21).

Of the OSCC samples included in this study, 35.03% (n= 62) included a para-tumor epithelium. The clone like distribution of ALDH1A1+ cells was detected in 56.6% of these samples (Figure 24).

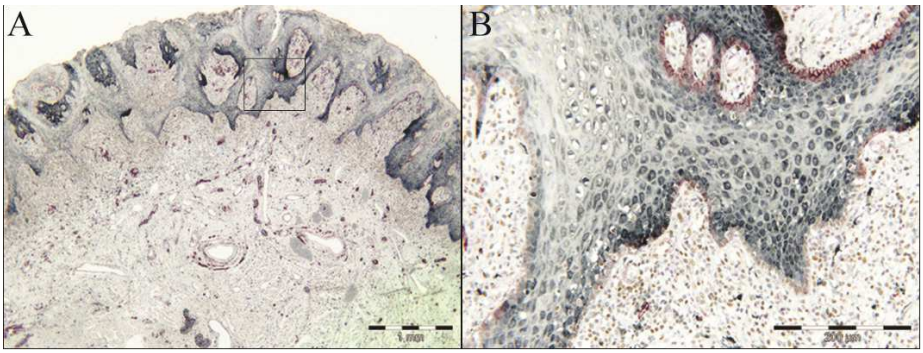

Figure 24: Representative example of para-tumor epithelium from the edge of an OSCC stained for CSC-related markers, BMI1 (brown), p75NTR (purple), ALDH1A1 (grey). Picture shows high expression of ALDH1A1 at the para-tumor epithelium.

5.2.4 OSCC samples that contained cells positive for the three CSC-related markers were rare

It is noteworthy here that five (2.8 %) OSCC samples showed no expression of any of the three markers by the tumor cells, despite the positivity of the internal controls, and that only 37.9% (n= 67) OSCC samples scored more than 0 for p75NTR and ALDH1A1 simultaneously. Co-localization of p75NTR or ALDH1A1 with BMI1 was detected in 58.2% (n= 103) and 52.5% (n= 93) respectively. Cells positive for both p75NTR and ALDH1A1 were detected only in 19.2% (n= 16) of all OSCC samples, and triple positive cells were detected in 18.1% of the samples (n=32) (Figure 22).

5.2.5 No difference between the tumor center and invading front or lymph nodes metastasis in the expression of the three CSC-related markers

Scores obtained from IHC for the three CSC-related markers from the tumor center were compared to tumor invading front (n=25) or metastatic lymph node tumors (n=19) as pairs (Figure 25A-D). No statistically significant difference was observed for any of the three markers investigated (Table 2, McNemar test).

			Tumor center			
			Low	High	Total	*p*-value
	ALDH1A1					
Invading front	**ALDH1A1**	Low	19 (100%)	5 (100%)	24 (100%)	ND
		High	0	0	0	
	p75NTR					
	p75NTR	Low	15 (88.2%)	6 (85.7%)	21 (87.5%)	0.289
		High	2 (11.8%)	1 (14.3%)	3 (12.5%)	
	BMI1					
	BMI1	Low	5 (100%)	5 (26.3%)	10 (41.7%)	0.074
		High	0 (0.0%)	14 (73.7%)	14 (58.3%)	
	ALDH1A1					
Lymph node metastasis	**ALDH1A1**	Low	13 (100%)	3 (50.0%)	16 (84.2%)	0.248
		High	0 (0%)	3 (50.0%)	3 (15.8%)	
	p75NTR					
	p75NTR	Low	13 (86.7%)	1 (25.0%)	14 (73.7%)	1.000
		High	2 (13.3%)	3 (75.0%)	5(26.3%)	
	BMI1					
	BMI1	Low	3 (75.0%)	5 (33.3%)	8 (42.1%)	0.221
		High	1 (25.0.3%)	10 (66.7%)	9 (57.9%)	

Table 2: Comparison of the dichotomized IHC scores from three CSC-related markers, between the tumor center and invading front or lymph nodes metastasis, using McNemar test.

The expression levels of mRNA for p75NTR and ALDH1A1 was compared between laser micro-dissected pieces from the tumor center and tumor invading front in 23 OSCC samples. No reaction product was detected in some of the samples, and the pair-wise comparison was valid only in seven samples for ALDH1A1, and eight for p75NTR. No statistically significant difference was found (Figure 25E).

Although based on a small number of cases, these data indicated that the expression of the CSC-related markers investigated in this study was similar at the tumor center, invading front and lymph node metastasis.

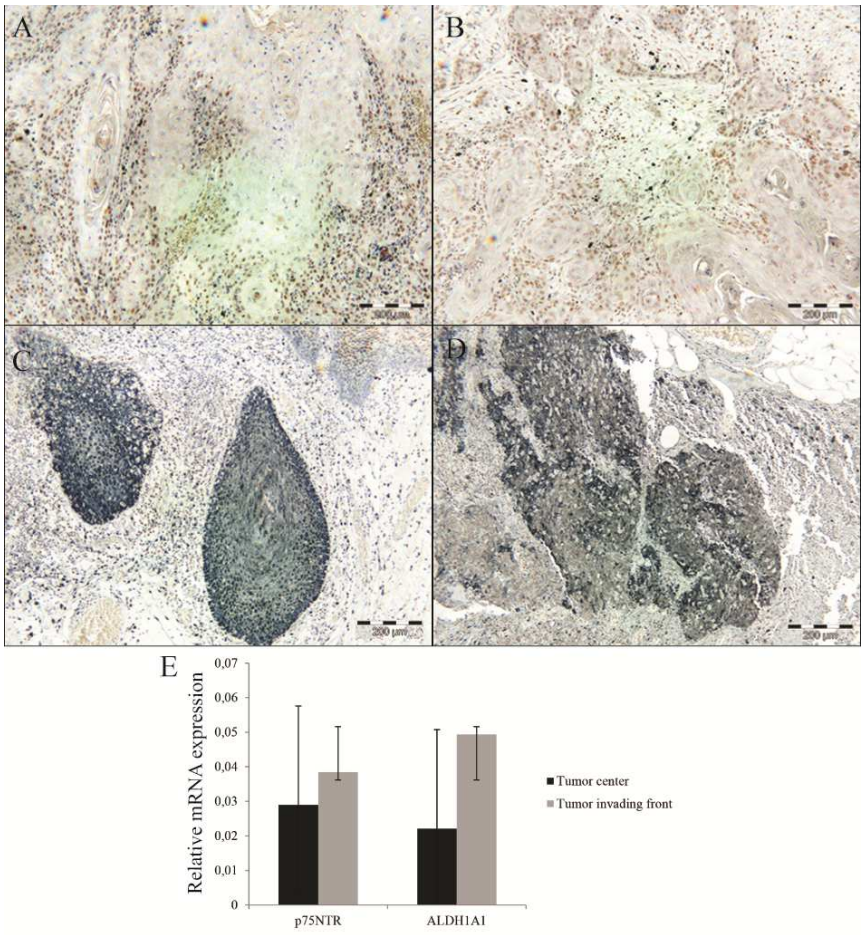

Figure 25: Representative two samples from OSCC subjected to triple IHC of CSC-related markers (A-D), BMI1 (brown), p75NTR (purple) and ALDH1A1 (grey). Pictures taken from tumor center (left) and lymph node metastasis (right). Bar chart comparing relative expression of p75NTR and ALDH1A1 in the tumor center and invading front (E). Error bars represents standard deviation.

5.2.6 Lack of co-localization and heterogeneously increased expression of CSC-related markers in *in vitro* OD and OSCC-derived cells

A step-wise increase in the expression of p75NTR at the protein level was found to follow the disease progression from NHOM, through OD to OSCC, despite the lack of $p75NTR^+$ cells in some OSCC samples. A similar change in the expression of

ALDH1A1 and CD44 was observed, although OD samples showed slightly higher expression levels. For all three CSC-related markers, the expression level was found to display wider ranges in OSCC and OD-derived cells when compared to NOKs (Figure 26 A-C, Table 3). However, these findings were found not be statistically significant (Kruscal-Wallis test).

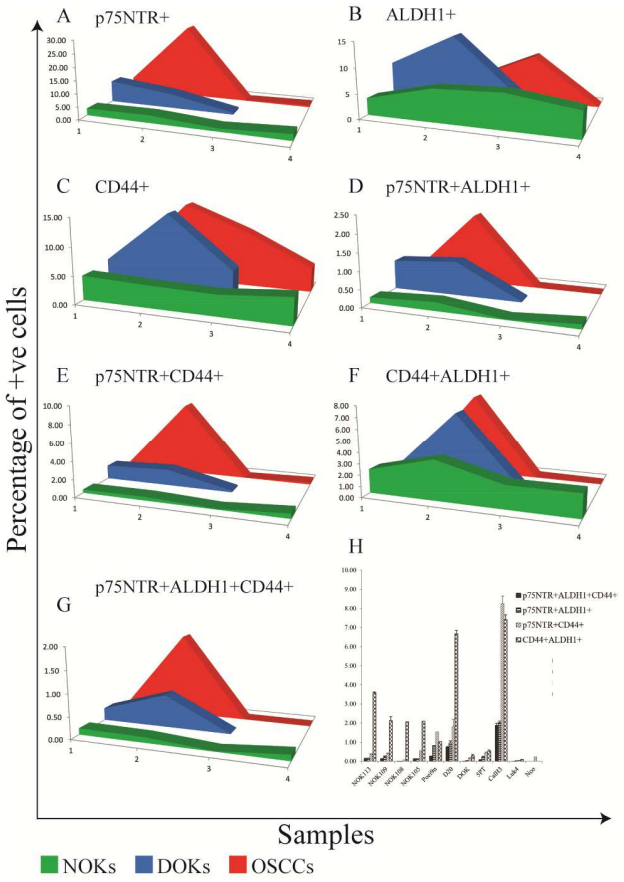

Figure 26: Area-under-the curve chart showing the expression levels, and frequency of co-localization of CSC-related markers in NOKs (n=4), OD (n=3) and OSCC (n=4) -derived cells.

	p75NTR+	ALDH1+	CD44+
NOK113	2.70 ± 0.00	6.57 ± 0.12	4.40 ± 0.78
NOK109	2.93 ± 0.23	7.03 ± 0.40	3.97 ± 0.25
NOK108	1.2 ± ND	3.4 ± ND	3.7 ± ND
NOK105	2.5 ± ND	5.2 ± ND	4.7 ± ND
Poei9n	8.5 ± ND	8.4 ± ND	5.1 ± ND
D20	5.7 ± 0.00	14.8 ± 0.14	14.45 ± 0.49
DOK	0.75 ± 0.07	3.35 ± 0.07	5.1 ± 0.14
5PT	5.3 ± 0.53	3.23 ± 0.06	3.17 ± 0.21
CaLH3	29.13 ± 0.55	9.7 ± 0.17	14.67 ± 0.49
LuC4	0.25 ± 0.07	3.85 ± 0.07	10.15 ± 0.21
Neo	0.7 ± ND	0 ± ND	4.4 ± ND

Table 3: Frequency of the three subpopulations (mean ± SD) in cells derived from NHOM (top), OD (middle) and OSCC (bottom) as examined by FACS analysis.

On the other hand, co-localization of pairs, or all the three of the CSC-related markers, was found to be more variable as the disease is progressing from normal to OSCC (Figure 26D-H, Table 4).

	p75NTR+ALDH1+	p75NTR+CD44+	CD44+ALDH1+	p75NTR+ALDH1+CD44+
NOK113	0.16 ± 0.01	0.37 ± 0.02	3.59 ± 0.04	0.14 ± 0.01
NOK109	0.25 ± 0.04	0.41 ± 0.03	2.13 ± 0.21	0.12 ± 0.02
NOK108	0.02 ± ND	0.07 ± ND	2.07 ± ND	0.01 ± ND
NOK105	0.14 ± ND	0.56 ± ND	2.10 ± ND	0.14 ± ND
Poei9n	0.83 ± ND	1.54 ± ND	1.04 ± ND	0.28 ± ND
D20	0.97 ± 0.10	1.82 ± 0.38	6.68 ± 0.16	0.74 ± 0.05
DOK	0.03 ± 0.00	0.17 ± 0.02	0.29 ± 0.06	0.01 ± 0.00
5PT	0.23 ± 0.03	0.45 ± 0.04	0.53 ± 0.06	0.07 ± 0.01
CaLH3	2.03 ± 0.08	8.25 ± 0.40	7.42 ± 0.24	1.88 ± 0.10
LuC4	0.01 ± 0.01	0.03 ± 0.01	0.09 ± 0.01	0.00 ± 0.00
Neo	0 ± ND	0.23 ± ND	0 ± ND	0 ± ND

Table 3: Frequency of co-localization (mean ± SD) of the three subpopulations in cells derived from NHOM (top), OD (middle) and OSCC (bottom) as examined by FACS analysis.

5.2.7 Increased proliferation in p75NTR+ OSCC cells compared to ALDH1

Comparison of the mean percentages of proliferating cells within p75NTR+, ALDH1A1+ and p75NTR+ALDH1A1+ cell subpopulations was performed for NHOM (n=19) and OSCC samples (n= 58) (Figure 27A,B). Friedman test revealed a significant difference between the percentages of proliferating cells in the three cell subpopulations in NHOM (P-value= 0.006) as well as in OSCC (P-value= 0.000), and a higher percentage of proliferating cells was observed in p75NTR+ subpopulation. Further comparison of pairs of the three cell subpopulations using Wilcoxon-Rank test (Figure 27C,D) revealed a significant difference between p75NTR+ and ALDH1A1+ in NHOM (P-value= 0.005) and OSCC (P-value= 0.000). Another statistically significant difference was found between p75NTR+ and p75NTR+ALDH1A1+ subpopulations in NHOM (P-value= 0.008) and in OSCC (P-value= 0.000), but not between ALDH1A1+ and p75NTR+ALDH1A1+ subpopulations neither in NHOM (P-value= 0.217) nor in OSCC (P-value= 0.273).

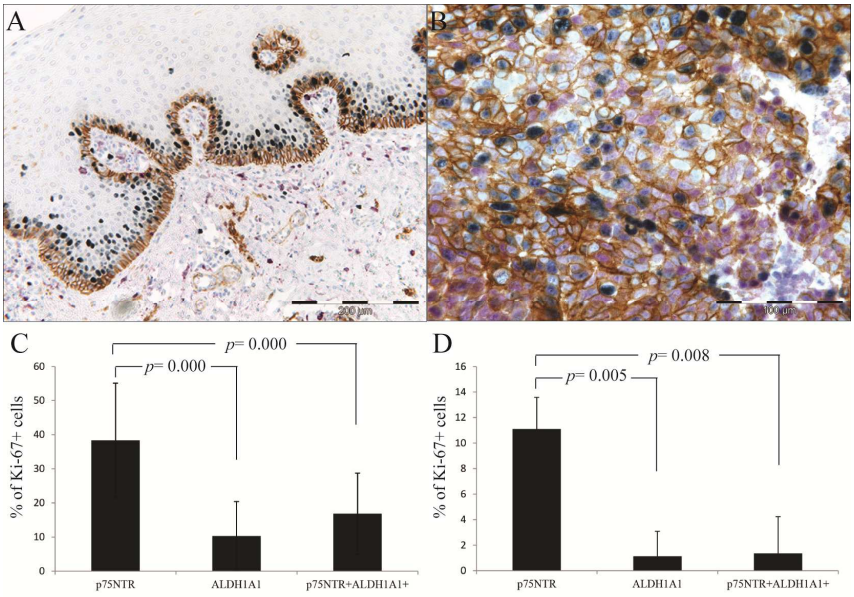

Figure 27: Representative examples from NHOM (A) and OSCC (B) subjected to triple IHC for p75NTR (brown), ALDH1A1 (purple) and Ki-67 (gray). Bar charts comparing the frequency of proliferating cells in the three subpopulations in OSCC (B) and NHOM (C).

5.2.8 High expression of p75NTR and ALDH1A1 in OSCC correlated with different clinical parameters

High expression of p75NTR was found to be associated with small size tumors, and tumors graded as low-moderately differentiated (0.034 for both, Chi-Square test). Kaplan-Meier`s curve showed that patients with high p75NTR expressing tumors are more likely to survive shorter within a period of 10 years (Figure 28A), but the finding was not statistically significant (Tarone-Ware test). Stratifying the same analysis by tumor size revealed a similar difference in the survival probabilities in patients with T1-T2 tumors, but not in patients with T3-T4 tumors (Figure 28B,C).

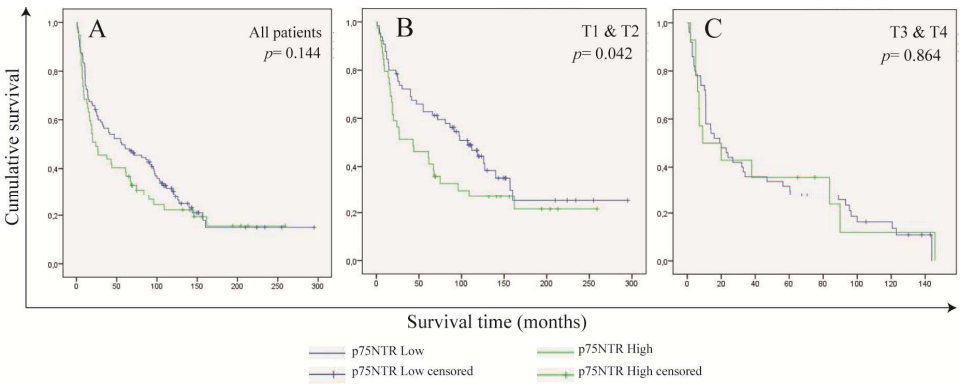

Figure 28: Kaplan-Meier`s curves showing the difference in survival probabilities between between OSCCs with high or low frequency of p75NTR+ cells. The analysis was conducted for all cases (A), for T1 & T2 (B) and T3 & T4(C) OSCCs.

Despite the lack of statistical significance, Cox regression hazard models revealed similar survival pattern, and a marked change in the hazard ratio was observed when the analysis was adjusted by the tumor size (Table 4).

Model	Overall sig.	covariate	Co-efficient (B)	Sig.	Exp(B)	HR
Crude	0.247	p75NTR	- 0.213	0.248	0.808	1.24
Splitting data by Tumor size						
T1 & T2	0.088	p75NTR	- 0.418	0.09	0.658	1.52
T3 & T4	0.966	p75NTR	- 0.015	0.966	1.015	1.03
Adjusted for tumor size	0	p75NTR	- 0.4	0.104	0.67	1.49
		Tumor size	0.087	0.091	1.796	1.796
		Interaction	0.862	0.403	1.407	1.407

Table 4: Cox regression hazard models containing p75NTR as the only co-variate (Top), when the data were split by tumor size (middle) and when p75NTR, Tumor size and their interaction variable as co-variates.

On the other hand, high ALDH1A1 expression was found to be associated with lymph nodes metastasis (0.035, Chi-Square test). These data show that p75NTR and ALDH1A1 expression affect different aspects of the disease progression at different stages of the disease.

5.3 p75NTR^{High} OSCC-derived cells displayed several characteristics previously related to the CSC-phenotype (Paper III)

Cells sorted according to p75NTR expression were subjected to different CSC assays. The percentage of p75NTR^{High} cells that formed spheres or colonies (Figure 29) were found to be 4.14% ± 1.28 and 44% ± 2.58 respectively, compared to only 1.7% ± 0.58 and 25.3% ± 3.4 for p75NTR^{Low} cells. These data show that higher percentage of the seeded p75NTR^{High} CaLH3 cells formed colonies and spheres with a statistically significant difference, as compared to p75NTR^{Low} cells (p= 0.000, Mann-Whitney test).

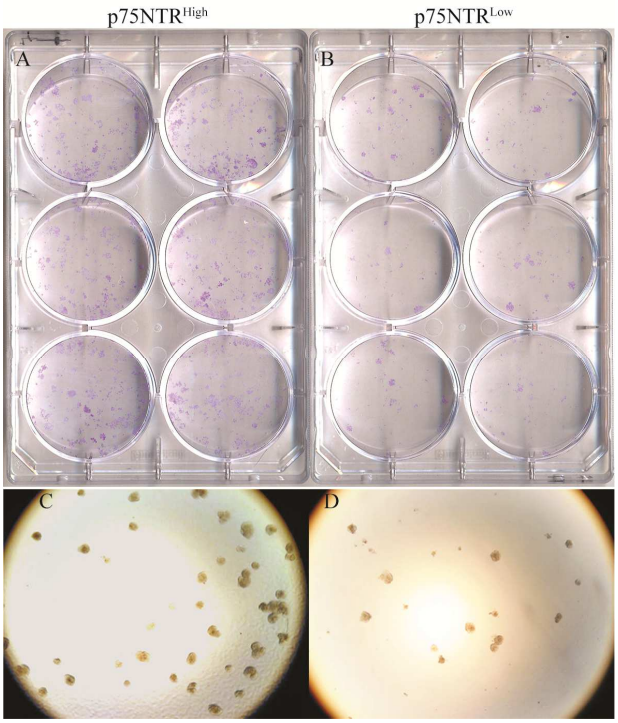

Figure 29: Representative images of colony (upper) and sphere (lower) formation assays for p785NTR^{High} (left) and p75NTR^{Low} (right) CaLH3 cells.

The incidence of tumor formation was found to be higher in mice injected with p75NTR^{High} cells than in mice injected with p75NTR^{Low} cells (90%, 70% respectively). The highest difference in tumor formation incidence was observed at the first reading (70% for p75NTR^{High} compared to 30% for p75NTR^{Low}). Pair wise comparison of the mean tumor size

between the two animal groups at each of the time points, showed that tumors generated by p75NTR^{High} cells were growing significantly bigger (P-value = 0.043, Wilcoxon Signed Rank Test). However, IHC for Ki-67 showed no difference in the percentage of proliferating cells between the two animal groups. Instead, a difference in the expression of involucrin was detected by digital image analysis of sections subjected to IHC for that differentiation marker. These data show a shorter lag phase and higher growth rate of xenografts (Figure 30) generated by p75NTR^{High} cells at their early stages.

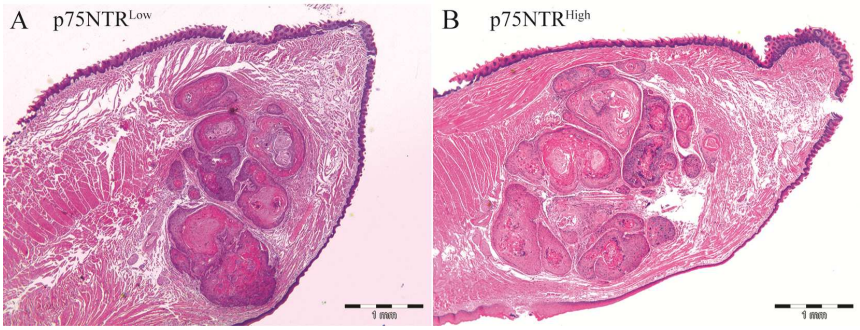

Figure 30: Representative images of xenograft models generated by transplantation of p75NTR^{Low} (A) and p75NTR^{High} CaLH3 cells into NSG mouse tongue.

Additionally, cell cycle analysis (Figure 31) showed that a higher proportion of p75NTR^{High} cells (32.07% ± 9.2) were found to be at G2 phase compared to p75NTR^{Low} (8.91% ± 3.34) and the unsorted CaLH3 population (22.15% ± 9.02) . The p75NTR^{High} cells were also found to be more resistant to 5-Fluorouracil than p75NTR^{Low} cells as evident by the drug resistance experiment.

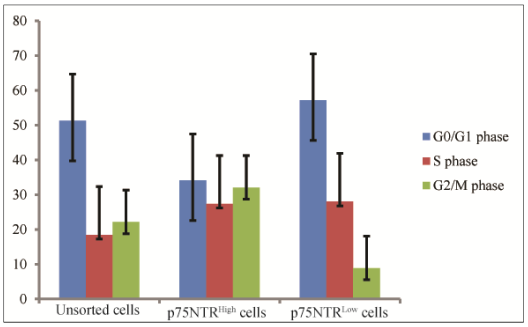

Figure 31: Bar chart displaying cell cycle distribution of CaLH3 cells sorted for p75NTR expression or not. Error bars represents standard deviation.

5.4 Subpopulations of p75NTR^{High} and ALDH^{br} cells displayed different expression profile of CSC and EMT related molecules (Paper II)

Both p75NTR^{High} and ALDH1^{br} were found to have higher expression of surface markers previously related to CSCs in OSCC, as compared to their negative counterparts by qRT-PCR. Nonetheless, the gene POU5F1 was found to be higher expressed by ALDH1^{di} cells as compared to ALDH1^{br} cells, while inverse pattern was detected in cells sorted for p75NTR expression. The EMT marker vimentin was found to be upregulated in ALDH1^{br} cells but not in p75NTR^{High} cells. Additionally, expression pattern of differentiation markers (CK-13 and involucrin) indicated that ALDH1^{br} cells are more differentiated than their negative counterpart (Figure 32).

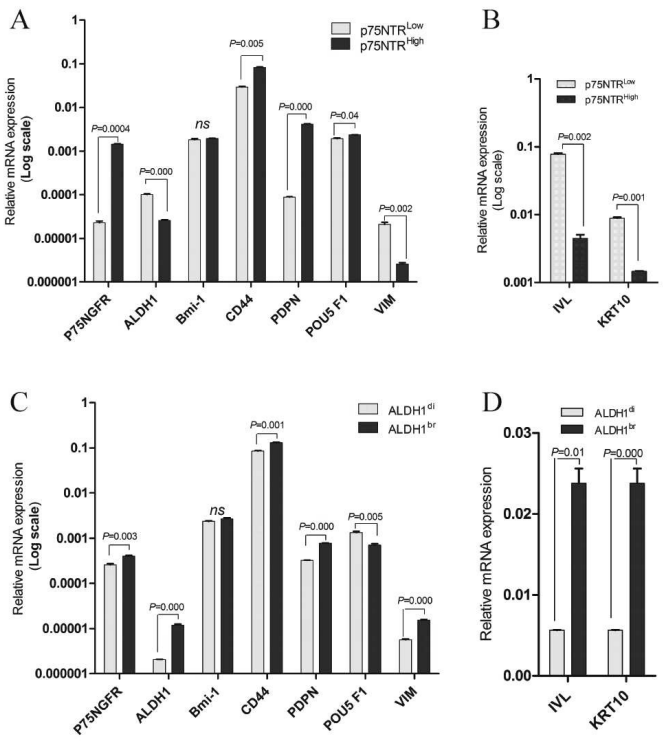

Figure 32: Bar Charts representing relative mRNA expression levels of CSC and EMT related markers (left) and differentiation markers (right), for cells sorted for p75NTR (A,B) or ALDH1 (C,D) expression.

5.5 Subpopulations of p75NTR^{High} and ALDH1^{br} OSCC-derived cells could spontaneously arise from a more differentiated subpopulation (Paper II)

Cells sorted for p75NTR or ALDH1 expression were propagated in culture for a week, and the FACS analysis was performed as before. Based on the concomitant negative control, cells propagated from p75NTR^{High} were found to contain 40.1% p75NTR^{Low} cells. While 8.06% p75NTR^{High} were detected within cells propagated from p75NTR^{Low}.

Similar observation was made when xenografts generated from p75NTR^{Low} CaLH3 cells were compared to the ones generated from p75NTR^{High} cells, and IHC showed no difference in the number of p75NTR+ cells.

Propagation of cells sorted for ALDH1 activity for the same period of time as for p75NTR^{High} cells, showed that cells propagated from ALDH1^{br} included 97.73 ALDH1^{di}. On the other hand, 0.17% ALDH1^{br} were found to arise from propagation of ALDH1^{di} cells. These data show that p75NTRHigh and ALDH1br OSCC-derived cells can arise *de novo* spontaneously in culture (Figure 33).

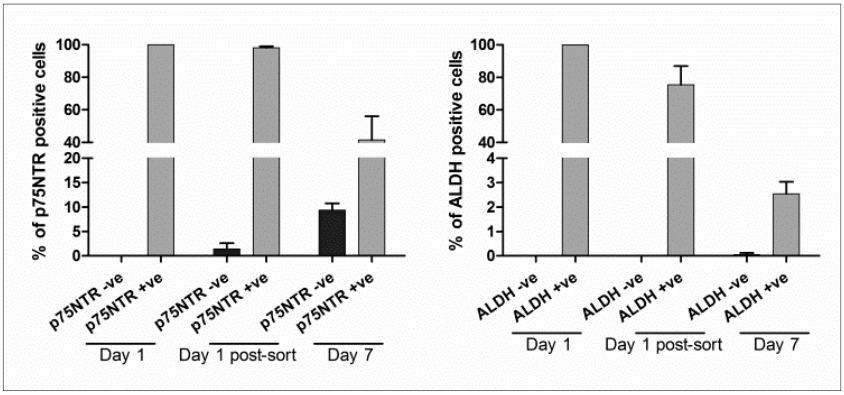

Figure 33: Bar chart displaying postsort checking and percentage of positive cells arising de nove after propagation in culture.

6. Discussion

6.1 Variability in the expression of CSC-related markers in patients with OD and OSCC as compared to NHOM

Variability in the expression of CSC-related markers has been previously reported and high expression levels have been correlated to patients prognosis in melanoma (159), colorectal (57) and breast cancers (160), glioma (161) and OSCC (111). In AML, the frequency of $ALDH1^+$ cells was found to vary from 1-16% (104). Another study found that $CD34^+CD38^-$ varied by 1000 folds in a cohort of 16 patients (162). In OSCC primary cells, CD44+ cells varied from 0.1% to 41.72% (105). Another study found an increase in the expression of several CSC-related markers in OSCC-derived cell lines in comparison to ones derived from OD or NHOM (149). Nevertheless, correlation between the degree of this variability and the progression of disease has not been addressed so far. In this project, expression of p75NTR and ALDH1A1 in OD and OSCC was found to be increased in comparison to NHOM, and high expression was found to be associated with poor prognosis and less survival chances of OSCC patients, which is in agreement with previous reports. However, the widely scattered level of expression of all three CSC related markers observed in OD and OSCC as compared to NHOM is one of the key new findings. Cells positive for p75NTR, for example, comprised more than 50% in some OSCCs, a high frequency that was not detected in any of the NHOM samples, while other OSCCs contained <1% p75NTR+ cells. The distribution of cells positive for CSC-related markers was also found to be heterogeneous in OSCC and OD as compared in NHOM. In fact, loss of spatial regulation of CD44 and p75NTR was reported before in an OSCC *in vitro* 3D model, but not in parallel stepwise models constructed for NOKs or OD-derived cells (149). This variability in expression and distribution may be due to differences in the genetic background of the disease and/or in the tumor microenvironment. The lack of expression of all three CSC-related markers observed in some of OSCC in this study (n= 5), indicates that progression of these tumors is driven by another phenotype that

does not oblige BMI1 involvement. Perhaps these tumors are not hierarchically organized and all.

6.2 Multiple CSC subpopulations

Investigations on CSC from different models often yielded variable findings. In AML, leukemic stem cells were first identified as CD34+CD38- (54, 55). Other studies have reported CD34- subpopulation to contain leukemic stem cells (163, 164). Additionally, CD34+ALDH1^{br} subpopulation was also found to enrich in leukemic stem cells (104) as well as in the side population (165, 166). The same can be concluded for some solid tumors. In breast cancer, CSC have been descried as expressing CD44+CD24- (56). Later on, CSC activity was detected within the ALDH1 and this subpopulation was found to have only 1% overlapping with CD44+ subpopulation (98). In melanoma, CSC were first identified as p75NTR+ (167) but later on CSC have been identified within p75NTR- subpopulation (168). In OSCC, CSCs were first identified by use of CD44 (105), then ALDH1 bright subpopulation was also found to exhibit stem cell properties and to overlap with CD44^{high} subpopulation (101). Such inconsistencies between studies on the same tumor type can be due to difference in the experimental conditions, with underestimation of phenotypes that are potentially tumorigenic resulting from non-permissive experimental conditions. These conditions include the xenogenic immune barrier, as well as differences in the microenvironment (50). Another point of view attributes such difference in the phenotype of the tumorigenic cells to differences in the genetic background, cell of origin, site of tumor, histological subtype, microenvironment and time point [reviewed (50, 92, 154)]. However, it has been shown in pancreatic cancer, that there might be more than one CSC subpopulation within the same tumor (169). In this project, we found that p75NTR^{High} cells displayed more CSC properties than the p75NTR^{Low} cells. However, p75NTR^{Low} cells also seemed to contain few cells with CSC properties. In addition, our data showed that the overlap between p75NTR and ALDH1A1 is a rare finding both in patient materials and OSCC cells, and these two subpopulations seemed to be two separate subpopulations, minimally intersecting. This was also supported by

performing qRT-PCR on sorted CaLH3 cells, where $p75NTR^{Low}$ cells were found to express higher levels of ALDH1A1 as compared to $p75NTR^{High}$ cells, and vice versa.

Phenotypical differences between CSCs often reflected functional differences in many models. In inflammatory breast cancer, ALDH1+ CSCs were correlated to metastasis while CD44+CD24- CSCs were found to be highly proliferative (160). Similar observations were made in OSCC (119), where $CD44^{high}ESA^{high}$ cells were found to comprise the proliferative compartment, while $CD44^{high}ESA^{low}$ were the EMT compartment. In pancreatic adenocarcinoma, only CD133+CXCR4+ cells comprised the metastatic phenotype, and not the rest of CD133+ cells (169). Even normal hematopoietic stem cells have been classified into long term self-renewing, short-term self-renewing and multipotent progenitors without detectable self-renewal potential organized respectively in a hierarchy (63). In our samples, multiple IHC has showed that p75NTR+ cells were more proliferative than ALDH1A1+ cells, and p75NTR+ALDH1A1+ cells. This finding was in line with the suggested proliferation promoting role of p75NTR in mouse embryonic stem cells (29). We also found p75NTR expression to be correlated with less survival chances in patients with small size tumors. In addition, OSCC cells with high p75NTR expression exhibited higher resistance to 5-Fluorouracil as compared to $p75NTR^{Low}$ subpopulation. On the other hand, $ALDH1^{br}$ cells were found to express higher levels of the EMT-related marker vimentin. High expression for ALDH1A1 was also found to be associated with occurrence of lymph node metastasis. This is in line with previous studies showing a role of ALDH1+ OSCC cells in invasion (119), and reported the presence of those cells at the tumor invading front (106). In the current project, no difference in the expression level of ALDH1A1 or p75NTR between the tumor center and the invading front was observed. This can be due to the small sample size available for analysis. Although further functional investigation is needed, we theorize that these two subpopulations have different functions.

6.3 A role for cancer cell plasticity in *de novo* emergence of p7NTR^{high} and ALDH1^{br} cells

Our data showed that p75NTR+ and ALDH1+ cells could arise *de novo* in culture from a generally more differentiated subpopulation, and we described this phenomenon to occur also *in vivo* for p75NTR ^{high} cells. A possible explanation of this can be that these cells arise from another rare CSC population lurking within the negative compartment. In OSCC, CSCs were previously shown to have the ability to switch between two CSC phenotypes, an epithelial one and an EMT one positive for ALDH1 (119). In the present study, only partial overlap was found between p75NTR+, ALDH1+ and CD44+. This shows that a subpopulation that is negative for one of the three markers would contain cells positive for the two other markers. We have not investigated the generation of, for example, p75NTR+ cells from CD44+p75NTR- cells, and therefore, this explanation remains to be proven. Another explanation would be by the generation of p75NTR+ or ALDH1+ cells from the more differentiated, non-CSC, negative progeny by undergoing de-differentiation. This was shown in breast cancer, and mathematical modelling indicated that CSCs could arise stochastically from more differentiated breast cancer subpopulations (115). In fact, induction of de-differentiation of adult somatic cells into a pluripotent stem cell has already been performed (9), but under the influence of defined factors and the process was thought to involve reversion of epigenetic modifications (170).

Although we described *de novo* alteration of the phenotype that we observed both in culture and *in vivo* as 'spontaneous', one might argue that those conditions were stress conditions since selecting for only one phenotype of cells might have disturbed the equilibrium that might exist in a tumor at a certain point between multiple, phenotypically diverse cell subpopulations. It has been argued that cells with CSC properties may arise as result of high plasticity of the tumor cells in response to signals from the tumor microenvironment. Therefore, hypothetically it has been argued that any cell in a tumor can display CSC properties (50). Mathematical modelling showed also that tumorigenic behavior is a rather probabilistic potential of all tumor cells (171), and using a very permissive mouse model, it was found that any cell in some

melanomas can be a CSC (116). It was also suggested that tumor growth of melanoma is dependent on a temporary distinct subpopulation that is generated by turning on and off a histone demethylase (172). Subpopulations with therapy resistance were also suggested to arise reversibly from drug sensitive cells (173). Our data revealed a statistically significant association between high p75NTR and small size tumors. We interpreted that the p75NTR activity might be required in small size tumors but turned off/ not of importance later in some patients. The need for multiple methods for identification/isolation of CSC

Given the variability of the CSC phenotype between patients with the same tumor type, multiplex methods for simultaneous detection of potential CSC markers are needed. Such methods might comprise a useful tool for investigation of the relationship between CSC markers identified in different reports in individual patients. In the future, such methods might be feasible for classifying patients for individualized cancer therapy. In the current study, we optimized a method for combining antibodies from same subclass, which is often an obstacle for researchers. Multiple IHC have the advantage of utilizing patient materials without the need to expose the cells to enforceable events during culture. In addition, it provides long lasting histological and topographical details. Sections subjected to this protocol were found analyzable using digital image analysis, which can make evaluation of a large number of samples less laborious to researchers.

7. Conclusions

7.1 Multiple IHC reported here was found useful to investigate the relationship between different subpopulations with potential CSC properties, and can be applied for the same purpose in other types of cancer.

7.2 Different patients with OSCC have different CSC-related marker profile. Expression of p75NTR and ALDH1A1 is apparently related to different aspects of OSCC progression.

7.3 Plasticity may play a role in generation of OSCC cells with CSC properties. p75NTR was found to identify a subpopulation of OSCC cells in a transient stem cell state. This subpopulation is more proliferative than ALDH1A1 and highly enriched in small size tumors.

8. Future perspectives

8.1 Comparison of p75NTR^{High} and ALDH1^{br} OSCC cells from different cell lines and primary OSCC cells, in terms of proliferation, invasion, drug resistance, tumorigenicity and plasticity.

8.2 Investigation of the CSC properties of p75NTR^{High}ALDH1^{br} cells.

8.3 Exploring the expression pattern of a wider spectrum of potential CSC markers simultaneously in larger sample size of patient material.

8.4 Applying the mathematical model reported before in Breast cancer (115), to investigate the fate, relationship and source of p75NTR^{High}ALDH1^{di}, p75NTR^{Low}ALDH1^{br} , p75NTR^{High}ALDH1^{br}, p75NTR^{Low}ALDH1^{di}.

8.5 Propagation of cells sorted for CSC-related marker with conditioned medium collected from the total population of the same cells, and observing the change in the regeneration of CSCs by cells in the negative compartment.

8.6 Gene expression profiling of the dye retaining OSCC cells.

References

1. Garant PR. Oral cells and tissues. Chicago: Quintessence Pub. Co; 2003. ix, 430 p. p.
2. Pecorino L. Molecular Biology of Cancer. 2nd ed. New York: Oxford University Press; 2008. 316 p.
3. Presland RB, Dale BA. Epithelial structural proteins of the skin and oral cavity: function in health and disease. Critical reviews in oral biology and medicine : an official publication of the American Association of Oral Biologists. 2000;11(4):383-408.
4. Alberts B, Johnson A, Lewis J, Raff M, Roberts K, Walter P. Molecular Biology of The Cell. New York: Garland Science; 2008. 1600 p.
5. Nakamura T, Endo K, Kinoshita S. Identification of human oral keratinocyte stem/progenitor cells by neurotrophin receptor p75 and the role of neurotrophin/p75 signaling. Stem Cells. 2007;25(3):628-38.
6. Allen TD, Potten CS. Fine-structural identification and organization of the epidermal proliferative unit. J Cell Sci. 1974;15(2):291-319.
7. Pietersen AM, van Lohuizen M. Stem cell regulation by polycomb repressors: postponing commitment. Curr Opin Cell Biol. 2008;20(2):201-7.
8. Boyer LA, Lee TI, Cole MF, Johnstone SE, Levine SS, Zucker JP, et al. Core transcriptional regulatory circuitry in human embryonic stem cells. Cell. 2005;122(6):947-56.
9. Takahashi K, Yamanaka S. Induction of pluripotent stem cells from mouse embryonic and adult fibroblast cultures by defined factors. Cell. 2006;126(4):663-76.
10. Liu S, Dontu G, Mantle ID, Patel S, Ahn NS, Jackson KW, et al. Hedgehog signaling and Bmi-1 regulate self-renewal of normal and malignant human mammary stem cells. Cancer Res. 2006;66(12):6063-71.
11. Park IK, Qian D, Kiel M, Becker MW, Pihalja M, Weissman IL, et al. Bmi-1 is required for maintenance of adult self-renewing haematopoietic stem cells. Nature. 2003;423(6937):302-5.
12. Mihic-Probst D, Kuster A, Kilgus S, Bode-Lesniewska B, Ingold-Heppner B, Leung C, et al. Consistent expression of the stem cell renewal factor BMI-1 in primary and metastatic melanoma. Int J Cancer. 2007;121(8):1764-70.
13. Brabletz T, Jung A, Spaderna S, Hlubek F, Kirchner T. Opinion: migrating cancer stem cells - an integrated concept of malignant tumour progression. Nat Rev Cancer. 2005;5(9):744-9.
14. Chenn A, Walsh CA. Regulation of cerebral cortical size by control of cell cycle exit in neural precursors. Science. 2002;297(5580):365-9.
15. Zechner D, Fujita Y, Hulsken J, Muller T, Walther I, Taketo MM, et al. beta-Catenin signals regulate cell growth and the balance between progenitor cell expansion and differentiation in the nervous system. Dev Biol. 2003;258(2):406-18.
16. Reya T, Clevers H. Wnt signalling in stem cells and cancer. Nature. 2005;434(7035):843-50.
17. Guruharsha KG, Kankel MW, Artavanis-Tsakonas S. The Notch signalling system: recent insights into the complexity of a conserved pathway. Nature reviews Genetics. 2012;13(9):654-66.
18. Liu J, Sato C, Cerletti M, Wagers A. Notch signaling in the regulation of stem cell self-renewal and differentiation. Current topics in developmental biology. 2010;92:367-409.
19. Bigas A, Espinosa L. Hematopoietic stem cells: to be or Notch to be. Blood. 2012;119(14):3226-35.
20. Lowell S, Jones P, Le Roux I, Dunne J, Watt FM. Stimulation of human epidermal differentiation by delta-notch signalling at the boundaries of stem-cell clusters. Curr Biol. 2000;10(9):491-500.

21. Kershner AM, Shin H, Hansen TJ, Kimble J. Discovery of two GLP-1/Notch target genes that account for the role of GLP-1/Notch signaling in stem cell maintenance. Proc Natl Acad Sci U S A. 2014;111(10):3739-44.
22. Watt FM. Role of integrins in regulating epidermal adhesion, growth and differentiation. The EMBO journal. 2002;21(15):3919-26.
23. Calenic B, Ishkitiev N, Yaegaki K, Imai T, Kumazawa Y, Nasu M, et al. Magnetic separation and characterization of keratinocyte stem cells from human gingiva. Journal of periodontal research. 2010;45(6):703-8.
24. Marhaba R, Zoller M. CD44 in cancer progression: adhesion, migration and growth regulation. Journal of molecular histology. 2004;35(3):211-31.
25. Harper LJ, Costea DE, Gammon L, Fazil B, Biddle A, Mackenzie IC. Normal and malignant epithelial cells with stem-like properties have an extended G2 cell cycle phase that is associated with apoptotic resistance. BMC Cancer. 2010;10:166.
26. Hayashi K, Storesund T, Schreurs O, Khuu C, Husvik C, Karatsaidis A, et al. Nerve growth factor beta/pro-nerve growth factor and their receptors in normal human oral mucosa. Eur J Oral Sci. 2007;115(5):344-54.
27. Aggarwal BB. Signalling pathways of the TNF superfamily: a double-edged sword. Nature reviews Immunology. 2003;3(9):745-56.
28. Tomellini E, Lagadec C, Polakowska R, Le Bourhis X. Role of p75 neurotrophin receptor in stem cell biology: more than just a marker. Cellular and molecular life sciences : CMLS. 2014.
29. Moscatelli I, Pierantozzi E, Camaioni A, Siracusa G, Campagnolo L. p75 neurotrophin receptor is involved in proliferation of undifferentiated mouse embryonic stem cells. Exp Cell Res. 2009;315(18):3220-32.
30. Smith-Thomas LC, Fawcett JW. Expression of Schwann cell markers by mammalian neural crest cells in vitro. Development. 1989;105(2):251-62.
31. Stemple DL, Anderson DJ. Isolation of a stem cell for neurons and glia from the mammalian neural crest. Cell. 1992;71(6):973-85.
32. Okumura T, Shimada Y, Imamura M, Yasumoto S. Neurotrophin receptor p75(NTR) characterizes human esophageal keratinocyte stem cells in vitro. Oncogene. 2003;22(26):4017-26.
33. David A, Robin R, Alasttair D, David H, Steward F. Muir's Textbook of Pathology. London: Edward Arnold Pub. Ltd.; 2008. 77-100 p.
34. Hanahan D, Weinberg RA. Hallmarks of cancer: the next generation. Cell. 2011;144(5):646-74.
35. Boyle P, Levin B, Cancer. IAfRo, Organization. WH. World cancer report 2008. Lyon Geneva: International Agency for Research on Cancer ; Distributed by WHO Press; 2008. 510 p.
36. Ferlay J, Soerjomataram I, Ervik M, Dikshit R, Eser S, Mathers C, Rebelo M, Parkin DM, Forman D, Bray, F (2013). GLOBOCAN 2012 v1.0, Cancer Incidence and Mortality Worldwide: IARC CancerBase No. 11 [Internet]. Lyon, France: International Agency for Research on Cancer. Available from http://globocan.iarc.fr.
37. Mehanna H, Paleri V, West CM, Nutting C. Head and neck cancer--Part 1: Epidemiology, presentation, and prevention. BMJ (Clinical research ed). 2010;341:c4684.
38. Warnakulasuriya S. Global epidemiology of oral and oropharyngeal cancer. Oral Oncol. 2009;45(4-5):309-16.
39. Regezi JA, Sciubba JJ, Jordan RCK. Oral Pathology: clinical pathologic correlations. 5th ed. missouri: Saunders Elsevier; 2008. 418 p.

40. Rogers SN, Lowe D, Fisher SE, Brown JS, Vaughan ED. Health-related quality of life and clinical function after primary surgery for oral cancer. The British journal of oral & maxillofacial surgery. 2002;40(1):11-8.
41. Vermorken JB, Remenar E, van Herpen C, Gorlia T, Mesia R, Degardin M, et al. Cisplatin, fluorouracil, and docetaxel in unresectable head and neck cancer. The New England journal of medicine. 2007;357(17):1695-704.
42. Bonner JA, Harari PM, Giralt J, Cohen RB, Jones CU, Sur RK, et al. Radiotherapy plus cetuximab for locoregionally advanced head and neck cancer: 5-year survival data from a phase 3 randomised trial, and relation between cetuximab-induced rash and survival. The lancet oncology. 2010;11(1):21-8.
43. Coleman MP, Gatta G, Verdecchia A, Esteve J, Sant M, Storm H, et al. EUROCARE-3 summary: cancer survival in Europe at the end of the 20th century. Annals of oncology : official journal of the European Society for Medical Oncology / ESMO. 2003;14 Suppl 5:v128-49.
44. Kowalski LP, Carvalho AL, Martins Priante AV, Magrin J. Predictive factors for distant metastasis from oral and oropharyngeal squamous cell carcinoma. Oral Oncol. 2005;41(5):534-41.
45. Soland TM, Brusevold IJ, Koppang HS, Schenck K, Bryne M. Nerve growth factor receptor (p75 NTR) and pattern of invasion predict poor prognosis in oral squamous cell carcinoma. Histopathology. 2008;53(1):62-72.
46. Leemans CR, Tiwari R, Nauta JJ, van der Waal I, Snow GB. Recurrence at the primary site in head and neck cancer and the significance of neck lymph node metastases as a prognostic factor. Cancer. 1994;73(1):187-90.
47. Myers JN, Greenberg JS, Mo V, Roberts D. Extracapsular spread. A significant predictor of treatment failure in patients with squamous cell carcinoma of the tongue. Cancer. 2001;92(12):3030-6.
48. da Silva SD, Hier M, Mlynarek A, Kowalski LP, Alaoui-Jamali MA. Recurrent oral cancer: current and emerging therapeutic approaches. Frontiers in pharmacology. 2012;3:149.
49. Hanahan D, Coussens LM. Accessories to the crime: functions of cells recruited to the tumor microenvironment. Cancer Cell. 2012;21(3):309-22.
50. Meacham CE, Morrison SJ. Tumour heterogeneity and cancer cell plasticity. Nature. 2013;501(7467):328-37.
51. Nowell PC. The clonal evolution of tumor cell populations. Science. 1976;194(4260):23-8.
52. Clarke MF, Dick JE, Dirks PB, Eaves CJ, Jamieson CH, Jones DL, et al. Cancer stem cells--perspectives on current status and future directions: AACR Workshop on cancer stem cells. Cancer Res. 2006;66(19):9339-44.
53. Allan AL. Cancer stem cells in solid tumors. New York: Humana Press; 2011. xvii, 475 p. p.
54. Lapidot T, Sirard C, Vormoor J, Murdoch B, Hoang T, Caceres-Cortes J, et al. A cell initiating human acute myeloid leukaemia after transplantation into SCID mice. Nature. 1994;367(6464):645-8.
55. Bonnet D, Dick JE. Human acute myeloid leukemia is organized as a hierarchy that originates from a primitive hematopoietic cell. Nat Med. 1997;3(7):730-7.
56. Al-Hajj M, Wicha MS, Benito-Hernandez A, Morrison SJ, Clarke MF. Prospective identification of tumorigenic breast cancer cells. Proc Natl Acad Sci U S A. 2003;100(7):3983-8.
57. O'Brien CA, Pollett A, Gallinger S, Dick JE. A human colon cancer cell capable of initiating tumour growth in immunodeficient mice. Nature. 2007;445(7123):106-10.

58. Singh SK, Hawkins C, Clarke ID, Squire JA, Bayani J, Hide T, et al. Identification of human brain tumour initiating cells. Nature. 2004;432(7015):396-401.
59. Collins AT, Berry PA, Hyde C, Stower MJ, Maitland NJ. Prospective identification of tumorigenic prostate cancer stem cells. Cancer Res. 2005;65(23):10946-51.
60. Ho MM, Ng AV, Lam S, Hung JY. Side population in human lung cancer cell lines and tumors is enriched with stem-like cancer cells. Cancer Res. 2007;67(10):4827-33.
61. Yang ZF, Ho DW, Ng MN, Lau CK, Yu WC, Ngai P, et al. Significance of CD90+ cancer stem cells in human liver cancer. Cancer Cell. 2008;13(2):153-66.
62. Fang D, Nguyen TK, Leishear K, Finko R, Kulp AN, Hotz S, et al. A tumorigenic subpopulation with stem cell properties in melanomas. Cancer Res. 2005;65(20):9328-37.
63. Reya T, Morrison SJ, Clarke MF, Weissman IL. Stem cells, cancer, and cancer stem cells. Nature. 2001;414(6859):105-11.
64. Shackleton M, Quintana E, Fearon ER, Morrison SJ. Heterogeneity in cancer: cancer stem cells versus clonal evolution. Cell. 2009;138(5):822-9.
65. Costea DE, Tsinkalovsky O, Vintermyr OK, Johannessen AC, Mackenzie IC. Cancer stem cells - new and potentially important targets for the therapy of oral squamous cell carcinoma. Oral Dis. 2006;12(5):443-54.
66. Blair A, Hogge DE, Ailles LE, Lansdorp PM, Sutherland HJ. Lack of expression of Thy-1 (CD90) on acute myeloid leukemia cells with long-term proliferative ability in vitro and in vivo. Blood. 1997;89(9):3104-12.
67. Huntly BJ, Shigematsu H, Deguchi K, Lee BH, Mizuno S, Duclos N, et al. MOZ-TIF2, but not BCR-ABL, confers properties of leukemic stem cells to committed murine hematopoietic progenitors. Cancer Cell. 2004;6(6):587-96.
68. Potten CS, Owen G, Booth D. Intestinal stem cells protect their genome by selective segregation of template DNA strands. J Cell Sci. 2002;115(Pt 11):2381-8.
69. Ding XW, Wu JH, Jiang CP. ABCG2: a potential marker of stem cells and novel target in stem cell and cancer therapy. Life Sci. 2010;86(17-18):631-7.
70. Bjerkvig R, Tysnes BB, Aboody KS, Najbauer J, Terzis AJ. Opinion: the origin of the cancer stem cell: current controversies and new insights. Nat Rev Cancer. 2005;5(11):899-904.
71. Rajaraman R, Rajaraman MM, Rajaraman SR, Guernsey DL. Neosis--a paradigm of self-renewal in cancer. Cell Biol Int. 2005;29(12):1084-97.
72. Sundaram M, Guernsey DL, Rajaraman MM, Rajaraman R. Neosis: a novel type of cell division in cancer. Cancer Biol Ther. 2004;3(2):207-18.
73. Alwaheeb S, Chetty R. Adenosquamous carcinoma of the pancreas with an acantholytic pattern together with osteoclast-like and pleomorphic giant cells. J Clin Pathol. 2005;58(9):987-90.
74. Baydar D, Amin MB, Epstein JI. Osteoclast-rich undifferentiated carcinomas of the urinary tract. Mod Pathol. 2006;19(2):161-71.
75. Balic M, Lin H, Young L, Hawes D, Giuliano A, McNamara G, et al. Most early disseminated cancer cells detected in bone marrow of breast cancer patients have a putative breast cancer stem cell phenotype. Clin Cancer Res. 2006;12(19):5615-21.
76. Odoux C, Fohrer H, Hoppo T, Guzik L, Stolz DB, Lewis DW, et al. A stochastic model for cancer stem cell origin in metastatic colon cancer. Cancer Res. 2008;68(17):6932-41.
77. Mani SA, Guo W, Liao MJ, Eaton EN, Ayyanan A, Zhou AY, et al. The epithelial-mesenchymal transition generates cells with properties of stem cells. Cell. 2008;133(4):704-15.
78. Donnenberg VS, Donnenberg AD. Multiple drug resistance in cancer revisited: the cancer stem cell hypothesis. Journal of clinical pharmacology. 2005;45(8):872-7.

79. Bao S, Wu Q, McLendon RE, Hao Y, Shi Q, Hjelmeland AB, et al. Glioma stem cells promote radioresistance by preferential activation of the DNA damage response. Nature. 2006;444(7120):756-60.
80. Oravecz-Wilson KI, Philips ST, Yilmaz OH, Ames HM, Li L, Crawford BD, et al. Persistence of leukemia-initiating cells in a conditional knockin model of an imatinib-responsive myeloproliferative disorder. Cancer Cell. 2009;16(2):137-48.
81. Jiang X, Zhao Y, Smith C, Gasparetto M, Turhan A, Eaves A, et al. Chronic myeloid leukemia stem cells possess multiple unique features of resistance to BCR-ABL targeted therapies. Leukemia. 2007;21(5):926-35.
82. Diehn M, Cho RW, Lobo NA, Kalisky T, Dorie MJ, Kulp AN, et al. Association of reactive oxygen species levels and radioresistance in cancer stem cells. Nature. 2009;458(7239):780-3.
83. Iwasaki H, Suda T. Cancer stem cells and their niche. Cancer Sci. 2009;100(7):1166-72.
84. Park TS, Donnenberg VS, Donnenberg AD, Zambidis ET, Zimmerlin L. Dynamic Interactions Between Cancer Stem Cells And Their Stromal Partners. Current pathobiology reports. 2014;2(1):41-52.
85. Calabrese C, Poppleton H, Kocak M, Hogg TL, Fuller C, Hamner B, et al. A perivascular niche for brain tumor stem cells. Cancer Cell. 2007;11(1):69-82.
86. Krishnamurthy S, Dong Z, Vodopyanov D, Imai A, Helman JI, Prince ME, et al. Endothelial cell-initiated signaling promotes the survival and self-renewal of cancer stem cells. Cancer Res. 2010;70(23):9969-78.
87. Donnenberg VS, Donnenberg AD, Zimmerlin L, Landreneau RJ, Bhargava R, Wetzel RA, et al. Localization of CD44 and CD90 positive cells to the invasive front of breast tumors. Cytometry Part B, Clinical cytometry. 2010;78(5):287-301.
88. Vermeulen L, De Sousa EMF, van der Heijden M, Cameron K, de Jong JH, Borovski T, et al. Wnt activity defines colon cancer stem cells and is regulated by the microenvironment. Nat Cell Biol. 2010;12(5):468-76.
89. Bickenbach JR. Identification and behavior of label-retaining cells in oral mucosa and skin. J Dent Res. 1981;60 Spec No C:1611-20.
90. Barrandon Y, Green H. Three clonal types of keratinocyte with different capacities for multiplication. Proc Natl Acad Sci U S A. 1987;84(8):2302-6.
91. Till JE, McCulloch EA, Siminovitch L. A STOCHASTIC MODEL OF STEM CELL PROLIFERATION, BASED ON THE GROWTH OF SPLEEN COLONY-FORMING CELLS. Proc Natl Acad Sci U S A. 1964;51:29-36.
92. Visvader JE, Lindeman GJ. Cancer stem cells in solid tumours: accumulating evidence and unresolved questions. Nat Rev Cancer. 2008;8(10):755-68.
93. Fang DD, Kim YJ, Lee CN, Aggarwal S, McKinnon K, Mesmer D, et al. Expansion of CD133(+) colon cancer cultures retaining stem cell properties to enable cancer stem cell target discovery. Br J Cancer. 2010;102(8):1265-75
94. Goodell MA, Brose K, Paradis G, Conner AS, Mulligan RC. Isolation and functional properties of murine hematopoietic stem cells that are replicating in vivo. J Exp Med. 1996;183(4):1797-806.
95. Duester G. Retinoic acid synthesis and signaling during early organogenesis. Cell. 2008;134(6):921-31.
96. Sophos NA, Vasiliou V. Aldehyde dehydrogenase gene superfamily: the 2002 update. Chem Biol Interact. 2003;143-144:5-22.
97. Huang EH, Hynes MJ, Zhang T, Ginestier C, Dontu G, Appelman H, et al. Aldehyde dehydrogenase 1 is a marker for normal and malignant human colonic stem cells (SC) and tracks SC overpopulation during colon tumorigenesis. Cancer Res. 2009;69(8):3382-9.

98. Ginestier C, Hur MH, Charafe-Jauffret E, Monville F, Dutcher J, Brown M, et al. ALDH1 is a marker of normal and malignant human mammary stem cells and a predictor of poor clinical outcome. Cell Stem Cell. 2007;1(5):555-67.
99. Douville J, Beaulieu R, Balicki D. ALDH1 as a Functional Marker of Cancer Stem and Progenitor Cells. Stem Cells Dev. 2008;18(1):17-25.
100. Deng S, Yang X, Lassus H, Liang S, Kaur S, Ye Q, et al. Distinct expression levels and patterns of stem cell marker, aldehyde dehydrogenase isoform 1 (ALDH1), in human epithelial cancers. PLoS One. 2010;5(4):e10277.
101. Clay MR, Tabor M, Owen JH, Carey TE, Bradford CR, Wolf GT, et al. Single-marker identification of head and neck squamous cell carcinoma cancer stem cells with aldehyde dehydrogenase. Head Neck. 2010;32(9):1195-201.
102. Storms RW, Green PD, Safford KM, Niedzwiecki D, Cogle CR, Colvin OM, et al. Distinct hematopoietic progenitor compartments are delineated by the expression of aldehyde dehydrogenase and CD34. Blood. 2005;106(1):95-102.
103. Pearce DJ, Taussig D, Simpson C, Allen K, Rohatiner AZ, Lister TA, et al. Characterization of cells with a high aldehyde dehydrogenase activity from cord blood and acute myeloid leukemia samples. Stem Cells. 2005;23(6):752-60.
104. Ran D, Schubert M, Pietsch L, Taubert I, Wuchter P, Eckstein V, et al. Aldehyde dehydrogenase activity among primary leukemia cells is associated with stem cell features and correlates with adverse clinical outcomes. Experimental hematology. 2009;37(12):1423-34.
105. Prince ME, Sivanandan R, Kaczorowski A, Wolf GT, Kaplan MJ, Dalerba P, et al. Identification of a subpopulation of cells with cancer stem cell properties in head and neck squamous cell carcinoma. Proc Natl Acad Sci U S A. 2007;104(3):973-8.
106. Sterz CM, Kulle C, Dakic B, Makarova G, Bottcher MC, Bette M, et al. A basal-cell-like compartment in head and neck squamous cell carcinomas represents the invasive front of the tumor and is expressing MMP-9. Oral Oncol. 2010;46(2):116-22.
107. Chen YC, Chen YW, Hsu HS, Tseng LM, Huang PI, Lu KH, et al. Aldehyde dehydrogenase 1 is a putative marker for cancer stem cells in head and neck squamous cancer. Biochem Biophys Res Commun. 2009;385(3):307-13.
108. Chen YC, Chang CJ, Hsu HS, Chen YW, Tai LK, Tseng LM, et al. Inhibition of tumorigenicity and enhancement of radiochemosensitivity in head and neck squamous cell cancer-derived ALDH1-positive cells by knockdown of Bmi-1. Oral Oncol. 2010;46(3):158-65.
109. Zhang P, Zhang Y, Mao L, Zhang Z, Chen W. Side population in oral squamous cell carcinoma possesses tumor stem cell phenotypes. Cancer Lett. 2009;277(2):227-34.
110. Yajima T, Ochiai H, Uchiyama T, Takano N, Shibahara T, Azuma T. Resistance to cytotoxic chemotherapy-induced apoptosis in side population cells of human oral squamous cell carcinoma cell line Ho-1-N-1. Int J Oncol. 2009;35(2):273-80.
111. Chiou SH, Yu CC, Huang CY, Lin SC, Liu CJ, Tsai TH, et al. Positive correlations of Oct-4 and Nanog in oral cancer stem-like cells and high-grade oral squamous cell carcinoma. Clin Cancer Res. 2008;14(13):4085-95.
112. Okamoto A, Chikamatsu K, Sakakura K, Hatsushika K, Takahashi G, Masuyama K. Expansion and characterization of cancer stem-like cells in squamous cell carcinoma of the head and neck. Oral Oncol. 2009;45(7):633-9.
113. Zhang Q, Shi S, Yen Y, Brown J, Ta JQ, Le AD. A subpopulation of CD133(+) cancer stem-like cells characterized in human oral squamous cell carcinoma confer resistance to chemotherapy. Cancer Lett. 2010;289(2):151-60.

114. Harper LJ, Piper K, Common J, Fortune F, Mackenzie IC. Stem cell patterns in cell lines derived from head and neck squamous cell carcinoma. J Oral Pathol Med. 2007;36(10):594-603.
115. Gupta PB, Fillmore CM, Jiang G, Shapira SD, Tao K, Kuperwasser C, et al. Stochastic state transitions give rise to phenotypic equilibrium in populations of cancer cells. Cell. 2011;146(4):633-44.
116. Quintana E, Shackleton M, Sabel MS, Fullen DR, Johnson TM, Morrison SJ. Efficient tumour formation by single human melanoma cells. Nature. 2008;456(7222):593-8.
117. Donnenberg AD, Hicks JB, Wigler M, Donnenberg VS. The cancer stem cell: cell type or cell state? Cytometry Part A : the journal of the International Society for Analytical Cytology. 2013;83(1):5-7.
118. Huang SD, Yuan Y, Liu XH, Gong DJ, Bai CG, Wang F, et al. Self-renewal and chemotherapy resistance of p75NTR positive cells in esophageal squamous cell carcinomas. BMC Cancer. 2009;9:9.
119. Biddle A, Liang X, Gammon L, Fazil B, Harper LJ, Emich H, et al. Cancer stem cells in squamous cell carcinoma switch between two distinct phenotypes that are preferentially migratory or proliferative. Cancer Res. 2011;71(15):5317-26.
120. Stewart JM, Shaw PA, Gedye C, Bernardini MQ, Neel BG, Ailles LE. Phenotypic heterogeneity and instability of human ovarian tumor-initiating cells. Proc Natl Acad Sci U S A. 2011;108(16):6468-73.
121. Astashkina A, Mann B, Grainger DW. A critical evaluation of in vitro cell culture models for high-throughput drug screening and toxicity. Pharmacology & therapeutics. 2012;134(1):82-106.
122. Marselli L, Thorne J, Ahn YB, Omer A, Sgroi DC, Libermann T, et al. Gene expression of purified beta-cell tissue obtained from human pancreas with laser capture microdissection. The Journal of clinical endocrinology and metabolism. 2008;93(3):1046-53.
123. Ahn YB, Xu G, Marselli L, Toschi E, Sharma A, Bonner-Weir S, et al. Changes in gene expression in beta cells after islet isolation and transplantation using laser-capture microdissection. Diabetologia. 2007;50(2):334-42.
124. Seeberger KL, Eshpeter A, Rajotte RV, Korbutt GS. Epithelial cells within the human pancreas do not coexpress mesenchymal antigens: epithelial-mesenchymal transition is an artifact of cell culture. Lab Invest. 2009;89(2):110-21.
125. Grinnell F. Fibroblast biology in three-dimensional collagen matrices. Trends in cell biology. 2003;13(5):264-9.
126. Costea DE, Dimba AO, Loro LL, Vintermyr OK, Johannessen AC. The phenotype of in vitro reconstituted normal human oral epithelium is essentially determined by culture medium. J Oral Pathol Med. 2005;34(4):247-52.
127. Costea DE, Johannessen AC, Vintermyr OK. Fibroblast control on epithelial differentiation is gradually lost during in vitro tumor progression. Differentiation. 2005;73(4):134-41.
128. Costea DE, Loro LL, Dimba EA, Vintermyr OK, Johannessen AC. Crucial effects of fibroblasts and keratinocyte growth factor on morphogenesis of reconstituted human oral epithelium. J Invest Dermatol. 2003;121(6):1479-86.
129. Yokota A, Takeuchi H, Maeda N, Ohoka Y, Kato C, Song SY, et al. GM-CSF and IL-4 synergistically trigger dendritic cells to acquire retinoic acid-producing capacity. Int Immunol. 2009;21(4):361-77.
130. Miller HR. Fixation and tissue preservation for antibody studies. Histochem J. 1972;4(4):305-20.
131. van der Loos CM. Immunoenzyme Multiple Staining Methods. UK: BIOS Scientific Publishers Limited; 1999. 118 p.

132. Werner M, Chott A, Fabiano A, Battifora H. Effect of formalin tissue fixation and processing on immunohistochemistry. Am J Surg Pathol. 2000;24(7):1016-9.
133. Song LB, Zeng MS, Liao WT, Zhang L, Mo HY, Liu WL, et al. Bmi-1 is a novel molecular marker of nasopharyngeal carcinoma progression and immortalizes primary human nasopharyngeal epithelial cells. Cancer Res. 2006;66(12):6225-32.
134. Koch LK, Zhou H, Ellinger J, Biermann K, Holler T, von Rucker A, et al. Stem cell marker expression in small cell lung carcinoma and developing lung tissue. Hum Pathol. 2008;39(11):1597-605.
135. Osman TA, Oijordsbakken G, Costea DE, Johannessen AC. Successful triple immunoenzymatic method employing primary antibodies from same species and same immunoglobulin subclass. European journal of histochemistry : EJH. 2013;57(3):e22.
136. Ross AH, Grob P, Bothwell M, Elder DE, Ernst CS, Marano N, et al. Characterization of nerve growth factor receptor in neural crest tumors using monoclonal antibodies. Proc Natl Acad Sci U S A. 1984;81(21):6681-5.
137. Gemenetzidis E, Elena-Costea D, Parkinson EK, Waseem A, Wan H, Teh MT. Induction of human epithelial stem/progenitor expansion by FOXM1. Cancer Res. 2010;70(22):9515-26.
138. Sternberger LA, Joseph SA. The unlabeled antibody method. Contrasting color staining of paired pituitary hormones without antibody removal. J Histochem Cytochem. 1979;27(11):1424-9.
139. Lewis Carl SA, Gillete-Ferguson I, Ferguson DG. An indirect immunofluorescence procedure for staining the same cryosection with two mouse monoclonal primary antibodies. J Histochem Cytochem. 1993;41(8):1273-8.
140. Chan A, Matias MA, Farah CS. A novel and practical method using HRP-polymer conjugate and microwave treatment for visualization of 2 antigens raised from the same or different species in paraffin-embedded tissues. Appl Immunohistochem Mol Morphol. 2011;19(4):376-83.
141. Lan HY, Mu W, Nikolic-Paterson DJ, Atkins RC. A novel, simple, reliable, and sensitive method for multiple immunoenzyme staining: use of microwave oven heating to block antibody crossreactivity and retrieve antigens. J Histochem Cytochem. 1995;43(1):97-102.
142. Hayry V, Makinen LK, Atula T, Sariola H, Makitie A, Leivo I, et al. Bmi-1 expression predicts prognosis in squamous cell carcinoma of the tongue. Br J Cancer. 2010;102(5):892-7.
143. Jin H, Pan Y, Zhao L, Zhai H, Li X, Sun L, et al. p75 neurotrophin receptor suppresses the proliferation of human gastric cancer cells. Neoplasia (New York, NY). 2007;9(6):471-8.
144. Chang B, Liu G, Xue F, Rosen DG, Xiao L, Wang X, et al. ALDH1 expression correlates with favorable prognosis in ovarian cancers. Mod Pathol. 2009;22(6):817-23.
145. van der Loos CM. Multiple immunoenzyme staining: methods and visualizations for the observation with spectral imaging. J Histochem Cytochem. 2008;56(4):313-28.
146. Mulrane L, Rexhepaj E, Penney S, Callanan JJ, Gallagher WM. Automated image analysis in histopathology: a valuable tool in medical diagnostics. Expert review of molecular diagnostics. 2008;8(6):707-25.
147. Gammon L, Biddle A, Fazil B, Harper L, Mackenzie IC. Stem cell characteristics of cell sub-populations in cell lines derived from head and neck cancers of Fanconi anemia patients. J Oral Pathol Med. 2011;40(2):143-52.
148. Gammon L, Biddle A, Heywood HK, Johannessen AC, Mackenzie IC. Sub-sets of cancer stem cells differ intrinsically in their patterns of oxygen metabolism. PLoS One. 2013;8(4):e62493.

149. Dalley AJ, Abdulmajeed AA, Upton Z, Farah CS. Organotypic culture of normal, dysplastic and squamous cell carcinoma-derived oral cell lines reveals loss of spatial regulation of CD44 and p75(NTR) in malignancy. J Oral Pathol Med. 2013;42(1):37-46.
150. Muntoni A, Fleming J, Gordon KE, Hunter K, McGregor F, Parkinson EK, et al. Senescing oral dysplasias are not immortalized by ectopic expression of hTERT alone without other molecular changes, such as loss of INK4A and/or retinoic acid receptor-beta: but p53 mutations are not necessarily required. Oncogene. 2003;22(49):7804-8.
151. Frese KK, Tuveson DA. Maximizing mouse cancer models. Nat Rev Cancer. 2007;7(9):645-58.
152. Hadler-Olsen E, Wetting HL, Rikardsen O, Steigen SE, Kanapathippillai P, Grenman R, et al. Stromal impact on tumor growth and lymphangiogenesis in human carcinoma xenografts. Virchows Arch. 2010;457(6):677-92.
153. Sano D, Myers JN. Xenograft models of head and neck cancers. Head Neck Oncol. 2009;1:32.
154. Liu S, Wicha MS. Targeting breast cancer stem cells. J Clin Oncol. 2010;28(25):4006-12.
155. Cheng L, Ramesh AV, Flesken-Nikitin A, Choi J, Nikitin AY. Mouse models for cancer stem cell research. Toxicologic pathology. 2010;38(1):62-71.
156. Shultz LD, Schweitzer PA, Christianson SW, Gott B, Schweitzer IB, Tennent B, et al. Multiple defects in innate and adaptive immunologic function in NOD/LtSz-scid mice. Journal of immunology (Baltimore, Md : 1950). 1995;154(1):180-91.
157. Pearson T, Greiner DL, Shultz LD. Humanized SCID mouse models for biomedical research. Current topics in microbiology and immunology. 2008;324:25-51.
158. Shen Z, Kauttu T, Cao J, Seppanen H, Vainionpaa S, Ye Y, et al. Macrophage coculture enhanced invasion of gastric cancer cells via TGF-beta and BMP pathways. Scandinavian journal of gastroenterology. 2013;48(4):466-72.
159. Schatton T, Murphy GF, Frank NY, Yamaura K, Waaga-Gasser AM, Gasser M, et al. Identification of cells initiating human melanomas. Nature. 2008;451(7176):345-9.
160. Charafe-Jauffret E, Ginestier C, Iovino F, Tarpin C, Diebel M, Esterni B, et al. Aldehyde dehydrogenase 1-positive cancer stem cells mediate metastasis and poor clinical outcome in inflammatory breast cancer. Clin Cancer Res.16(1):45-55.
161. Zeppernick F, Ahmadi R, Campos B, Dictus C, Helmke BM, Becker N, et al. Stem cell marker CD133 affects clinical outcome in glioma patients. Clin Cancer Res. 2008;14(1):123-9.
162. Eppert K, Takenaka K, Lechman ER, Waldron L, Nilsson B, van Galen P, et al. Stem cell gene expression programs influence clinical outcome in human leukemia. Nat Med. 2011;17(9):1086-93.
163. Taussig DC, Vargaftig J, Miraki-Moud F, Griessinger E, Sharrock K, Luke T, et al. Leukemia-initiating cells from some acute myeloid leukemia patients with mutated nucleophosmin reside in the CD34(-) fraction. Blood. 2010;115(10):1976-84.
164. Terpstra W, Prins A, Ploemacher RE, Wognum BW, Wagemaker G, Lowenberg B, et al. Long-term leukemia-initiating capacity of a CD34-subpopulation of acute myeloid leukemia. Blood. 1996;87(6):2187-94.
165. Wulf GG, Wang RY, Kuehnle I, Weidner D, Marini F, Brenner MK, et al. A leukemic stem cell with intrinsic drug efflux capacity in acute myeloid leukemia. Blood. 2001;98(4):1166-73.
166. Moshaver B, van Rhenen A, Kelder A, van der Pol M, Terwijn M, Bachas C, et al. Identification of a small subpopulation of candidate leukemia-initiating cells in the side population of patients with acute myeloid leukemia. Stem Cells. 2008;26(12):3059-67.

167. Civenni G, Walter A, Kobert N, Mihic-Probst D, Zipser M, Belloni B, et al. Human CD271-positive melanoma stem cells associated with metastasis establish tumor heterogeneity and long-term growth. Cancer Res. 2011;71(8):3098-109.
168. Held MA, Curley DP, Dankort D, McMahon M, Muthusamy V, Bosenberg MW. Characterization of melanoma cells capable of propagating tumors from a single cell. Cancer Res. 2010;70(1):388-97.
169. Hermann PC, Huber SL, Herrler T, Aicher A, Ellwart JW, Guba M, et al. Distinct populations of cancer stem cells determine tumor growth and metastatic activity in human pancreatic cancer. Cell Stem Cell. 2007;1(3):313-23.
170. Yamanaka S. Elite and stochastic models for induced pluripotent stem cell generation. Nature. 2009;460(7251):49-52.
171. Kern SE, Shibata D. The fuzzy math of solid tumor stem cells: a perspective. Cancer Res. 2007;67(19):8985-8.
172. Roesch A, Fukunaga-Kalabis M, Schmidt EC, Zabierowski SE, Brafford PA, Vultur A, et al. A temporarily distinct subpopulation of slow-cycling melanoma cells is required for continuous tumor growth. Cell. 2010;141(4):583-94.
173. Sharma SV, Lee DY, Li B, Quinlan MP, Takahashi F, Maheswaran S, et al. A chromatin-mediated reversible drug-tolerant state in cancer cell subpopulations. Cell. 2010;141(1):69-80.